AIMS Mathematics, 10(7): 16570–16596.
DOI:10.3934/math.2025742
Received: 22 May 2025
Revised: 4 July 2025
Accepted: 18 July 2025
Published: 23 July 2025

https://www.aimspress.com/journal/Math

Research article

Approximate multi-degree reduction of disk Wang-Bézier generalized ball curves via improved black-winged kite algorithm

Xia Wang[1], **Feng Zou**[1], **Weilin Zhang**[1] **and Huogen Yang**[1,2,*]

[1] School of Science, Jiangxi University of Science and Technology, Ganzhou, Jiangxi 341000, China

[2] Jiangxi Provincial Key Laboratory of Multidimensional Intelligent Perception and Control, Jiangxi University of Science and Technology, Ganzhou, Jiangxi 341000, China

* **Correspondence:** Email: yhg_98@jxust.edu.cn.

Abstract: This study proposed an efficient optimization approach for the degree reduction approximation of disk Wang-Bézier generalized ball (DWBGB) curves, utilizing an improved black-winged kite algorithm (IBKA). A constrained optimization model was developed based on the geometric characteristics of DWBGB curves, accompanied by a novel error metric for degree reduction evaluation. The original BKA was enhanced in three key aspects. First, a Sobol sequence paired with opposition-based learning was utilized to optimize the initial population distribution, markedly improving diversity and quality. Second, an adaptive spiral search mechanism was incorporated to bolster local exploitation. Third, the foraging strategy of the parrot algorithm was integrated to enhance global exploration and optimization efficiency. Evaluations conducted on the IEEE CEC-2020 benchmark test suite indicated that IBKA surpassed ten leading intelligent optimization algorithms in convergence speed, solution precision, and stability. When applied to DWBGB curve degree reduction across four test cases, IBKA demonstrated superior approximation accuracy and convergence stability compared to four representative algorithms. Relative to the original BKA, IBKA yielded improvements of 53.85%, 80.89%, and 36.18% in mean error, standard deviation, and minimum error, respectively, confirming its efficacy and superiority in addressing the multi-degree reduction problem for DWBGB curves.

Keywords: disk Wang-Bézier curve; multi-degree reduction approximation; black-winged kite algorithm; adaptive spiral strategy; parrot algorithm
Mathematics Subject Classification: 65D15, 65D17, 90C59

1. Introduction

In animation modeling and artistic shape design, high-degree Ball curves are plagued by significant data redundancy and computational inefficiency [1]. Degree reduction approximation techniques have been employed to substantially mitigate data processing complexity and resource consumption. Consequently, extensive research has been conducted on the degree reduction of high-degree Ball curves. Hu et al. thoroughly investigated degree reduction algorithms for Said-Ball and Wang-Ball curves [2], while Wu derived degree reduction formulas for Wang-Said generalized ball (WSGB) and Said-Bézier generalized ball (SBGB) curves [3]. Tan et al. introduced interval analysis to the WSGB curve framework, exploring the interval WSGB curve and its degree reduction algorithm [4]. Liu et al. developed an explicit multi-degree reduction approximation algorithm for SBGB curves, utilizing transformations between SBGB and Jacobi basis functions to achieve a one-step multi-degree reduction while preserving high-order endpoint constraints [5]. Additionally, Wang et al. proposed a degree reduction algorithm for Wang-Bézier generalized ball (WBGB) curves, though its applicability is limited for specific location parameters [6]. These studies have established a robust theoretical and practical foundation for advancing curve degree reduction algorithms.

As research on curve degree reduction deepens, disk curves, distinguished by their unique geometric properties, have emerged as a research hotspot. Lin et al. introduced the disk curve concept by substituting control points with disks [7], noting that equal disk radii yield the well-known equidistant curve. The degree reduction of disk curves is typically addressed by decomposing it into two subproblems: degree reduction of the center curve and the radius function. Chen et al. explored degree reduction for disk Bézier curves, applying optimal uniform approximation to the center curve and formulating the radius function's degree reduction as a linear programming problem [8]. Liu et al. proposed the disk q-Bézier curve and developed two optimal uniform degree reduction algorithms for the center curve using transformations between Chebyshev polynomials and q-Bernstein basis functions, while addressing the radius function's degree reduction through a perturbation-based constrained optimization approach [9].

However, traditional degree reduction methods are hindered by accuracy loss, high computational complexity, and limited applicability. Swarm intelligence (SI) optimization algorithms, characterized by simplicity, flexibility, and efficiency, have gained traction in solving complex optimization problems [10], making their application to curve degree reduction a promising research direction. For instance, Zou et al. propose a multi-strategy enhanced coati optimization algorithm (MSECOA) for Said-Ball curve degree reduction to improve geometric preservation and outperform existing algorithms in accuracy and efficiency [11]. Hu et al. applied the grey wolf optimizer (GWO) to address multi-degree reduction for SG-Bézier curves [12]. Cao et al. introduced an enhanced squirrel search algorithm (NOSSA), incorporating optimal neighborhood updates and quasi-oppositional learning, demonstrating its efficacy in optimizing Ball-Bézier curve degree reduction [13]. Furthermore, Hu et al. developed a degree reduction model for disk Wang-Ball curves, proposing a multi-strategy enhanced chameleon swarm algorithm (CCECSA) that integrates crossover optimization, elite-guided mechanisms, and competitive replacement strategies, successfully applied to disk Wang-Ball curve degree reduction [14]. Existing research highlights the significant advantages of SI algorithms in curve degree reduction, particularly for high-degree and complex curves.

The primary contributions of this study are delineated as follows:

- A degree reduction approximation model for the disk Wang-Bézier generalized ball (DWBGB) curve is proposed. Two objective functions are formulated: one minimizing the Euclidean distance and curvature error of the central curve, and another minimizing the radius deviation between the original and reduced curves. Additionally, a novel formula for degree reduction error is introduced.
- An improved black-winged kite algorithm (IBKA) is developed. The algorithm integrates the Sobol sequence and opposition-based learning method for population initialization, employs an adaptive spiral strategy to refine migration behavior, and incorporates the partial position update formula from the parrot optimization algorithm to address limitations of the original algorithm, thereby improving global search capability and optimization efficiency.
- The IBKA is applied to the DWBGB curve degree reduction approximation problem, resulting in a model based on IBKA. The algorithm's superiority is demonstrated through four numerical examples, each involving varying degrees of reduction, confirming its effectiveness in degree reduction of DWBGB curves.

The structure of the remainder of this paper is as follows: Section 2 discusses the degree reduction approximation problem of the DWBGB curve and presents the specific model. Section 3 elaborates on the IBKA in detail and conducts verification and analysis of this algorithm. In section 4, IBKA is used to approximate the DWBGB curve, and its superiority is verified by four numerical examples. Section 5 concludes the paper.

2. The degreee reduction approximation of DWBGB curves

2.1. DWBGB curves

Definition 1. *For a given natural number m, location parameter $L \in \{0, 1, \ldots, m\}$, and $n = 2m$ or $n = 2m + 1$, the n-th degree WBGB basis function [15] is defined as shown in Eq* (2.1)*:*

$$\omega_i^n(t, n, L) = \begin{cases} \binom{n-2L}{i} t^i (1-t)^{n-2L-i}, & 0 \le i \le m-L-1, \\ 2^{i-m+L} \binom{n-2L}{m-L} t^i (1-t)^{i+2}, & m-L \le i \le m-1, \\ 2^L \binom{n-2L}{m-L} t^{\lfloor n/2 \rfloor} (1-t)^{\lceil n/2 \rceil}, & i = m, \\ \omega_{n-i}(1-t, n, L), & m < i \le n, \end{cases} \tag{2.1}$$

where $\lfloor n \rfloor$ denotes the largest integer less than or equal to n, and $\lceil n \rceil$ refers to the smallest integer greater than or equal to n.

Let the control disk be defined as $(P_0) = (x_0, y_0)_{r_0} = \left\{(x, y) \in \mathbb{R}^2 \mid (x - x_0)^2 + (y - y_0)^2 \le r_0^2\right\}$, where (x_0, y_0) represents the center coordinates of (P_0), and r_0 denotes its radius.

Definition 2. *Given $n + 1$ control disks $(P_i) = (x_i, y_i)_{r_i}, i = 0, 1, \ldots, n$, the n-th degree DWBGB curve $(W)(t)$ is defined as shown in Eq* (2.2)*:*

$$(W)(t) = \sum_{i=0}^{n} \omega_i^n(t, n, L)(P_i) = \sum_{i=0}^{n} \omega_i^n(t, n, L)(x_i, y_i)_{r_i}, (0 \le t \le 1). \tag{2.2}$$

Specifically, when $L = 0$, $(W)(t)$ is a Bézier curve; when $L = m$, $(W)(t)$ is a Wang-Ball curve.

Besides, Eq (2.2) can be expressed as

$$(W)(t) = (C(t), R(t)), (0 \le t \le 1), \tag{2.3}$$

where $C(t)$ represents the center curve of $(W)(t)$, and $R(t)$ represents the radius function of $(W)(t)$.

$$\begin{aligned} C(t) = (x(t), y(t)) = (\sum_{i=0}^{n} \omega_i^n(t, n, L)x_i, \sum_{i=0}^{n} \omega_i^n(t, n, L)y_i,), \\ R(t) = \sum_{i=0}^{n} \omega_i^n(t, n, L)r_i. \end{aligned} \tag{2.4}$$

Figure 1 illustrates the center curves and the corresponding 7th-degree DWBGB curve under varying location parameters.

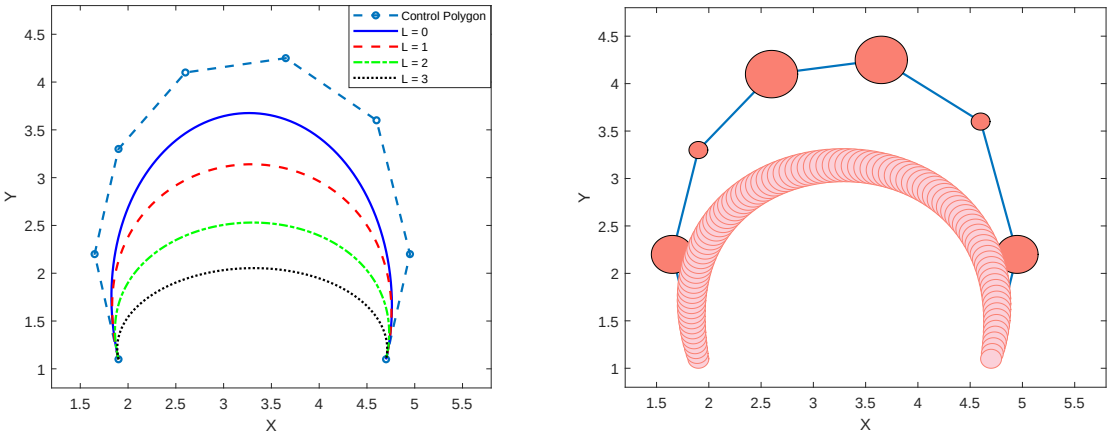

(a) Center curves **(b)** DWBGB curve($L = 1$)

Figure 1. 7th-degree DWBGB curve.

2.2. Degree reduction problem of DWBGB curves

The degree reduction approximation problem for DWBGB curves can be described as follows [16]: Given an n_1-th degree DWBGB curve $(P)(t) = (C_1(t), R_1(t))$, another DWBGB curve of n_2-th degree $(n_2 < n_1)$ is sought.

$$(Q)(t) = \sum_{i=0}^{n_2} \omega_i^{n_2}(t, n_2, L)(Q_i) = (C_2(t), R_2(t)). \tag{2.5}$$

The following condition must be satisfied:

$$(P)(t) \subseteq (Q)(t), 0 \le t \le 1, \tag{2.6}$$

and the width difference between $(P)(t)$ and $(Q)(t)$ should be minimized as much as possible.

Furthermore, Eq (2.6) can be expressed as Eq (2.7):

$$R_2(t) \ge R_1(t) + dist(C_1(t), C_2(t)), \tag{2.7}$$

where $dist(C_1(t), C_2(t)) = \| C_1(t) - C_2(t) \|_2$ represents the Euclidean distance between the original center curve $C_1(t)$ and the degree-reduced center curve $C_2(t)$.

The degree reduction problem for DWBGB curves is divided into two components: center curve degree reduction and radius function degree reduction.

2.2.1. Degree reduction of the center curve

The degree reduction of the center curve of a DWBGB curve is first formulated as an optimization problem. The objective function comprises two components: the first is the distance between curves $C_1(t)$ and $C_2(t)$, and the second is the curvature difference between $C_1(t)$ and $C_2(t)$. The center coordinates of the control disks for curve $C_2(t)$, denoted as $(x_{2,i}, y_{2,i})$, serve as the decision variables. The model is expressed as Eq (2.8):

$$\begin{aligned} &Minimize \quad F_1(C_2; C_1) = \tau \times \int_0^1 \|C_1(t) - C_2(t)\|^2 \, dt + (1-\tau) \times \int_0^1 (\kappa_1(t) - \kappa_2(t))^2 dt, \\ &\text{s.t.} \quad \begin{cases} x_{1,\min} - (x_{1,\max} - x_{1,\min}) \le x_{2,i} \le x_{1,\max} + (x_{1,\max} - x_{1,\min}), \\ y_{1,\min} - (y_{1,\max} - y_{1,\min}) \le y_{2,i} \le x_{1,\max} + (y_{1,\max} - y_{1,\min}), \end{cases} \quad i = 0, 1, \ldots, n, \end{aligned} \tag{2.8}$$

where τ denotes the weighting coefficient; $\kappa_1(t)$ and $\kappa_2(t)$ represent the curvatures of $C_1(t)$ and $C_2(t)$, respectively.

The curvature $\kappa(t)$ of the curve $C(t)$ is calculated as follows:

$$\kappa(t) = \frac{|x'(t)y''(t) - y'(t)x''(t)|}{(x'(t)^2 + y'(t)^2)^{\frac{3}{2}}}.$$

By appropriately defining the constraint range for the center coordinates of the control disks, the diversity of the population can be effectively maintained during the solution process of subsequent intelligent optimization algorithms. The terms $x_{1,\max}$ and $x_{1,\min}$ denote the maximum and minimum values, respectively, of the horizontal axis coordinates of the control disk centers for the original curve $P(t)$. Similarly, $y_{1,\max}$ and $y_{1,\min}$ represent the maximum and minimum values, respectively, of the vertical axis coordinates of the control disk centers.

The minimization of the objective function ensures that the curve $C_2(t)$ closely approximates the curve $C_1(t)$, while maintaining a high degree of shape consistency between them.

2.2.2. Degree reduction of the radius function

Similarly, the degree reduction problem for the radius function of a DWBGB curve can be formulated as an optimization problem, with its mathematical model expressed as Eq (2.9):

$$\begin{aligned} &Minimize \quad F_2(R_2; R_1) = \int_0^1 R_2^2(t) dt - \lambda \times \int_0^1 \min\left[R_2(t) - R_1(t) - dist(C_1(t), C_2(t)), 0\right] dt, \\ &s.t \quad r_{1,\min} \le r_{2,i} \le r_{1,\max} + 3d_{\max}, \quad i = 0, 1, \ldots, n_2, \end{aligned} \tag{2.9}$$

where $r_{1,\max}$ and $r_{1,\min}$ denote the maximum and minimum values, respectively, of the control disk radii for the curve $P(t)$. Establishing this constraint range facilitates maintaining population diversity during subsequent solutions based on intelligent optimization algorithms. The term $d_{\max}$ represents the maximum value of $dist(C_1(t), C_2(t))$, and λ is the weighting factor, which should be set as large as possible.

The minimization of the objective function $F_2(R_2; R_1)$ aims to ensure that the radius function $R_2(t)$ is as small as possible while satisfying the constraints specified in Eq (2.7).

2.2.3. Degree reduction error

To facilitate the comparison of different algorithms' performance in degree reduction, the proposed degree reduction error formula is employed for evaluation. In traditional methods for degree reduction approximation of disk curves, the infinity norm is commonly used to measure approximation error [8], which only captures the maximum local deviation while neglecting the overall error distribution, thus failing to comprehensively characterize the approximation quality. To address this, a degree reduction error formula is defined as shown in Eq (2.10):

$$e = \int_0^1 |R_1(t) - R_2(t)| + |dist(C_1(t), C_2(t))|dt. \tag{2.10}$$

3. IBKA

3.1. BKA

The BKA is a novel metaheuristic optimization algorithm inspired by the unique attack and migration behaviors of the black-winged kite [17].

3.1.1. Attacking behavior

The attack behavior of the black-winged kite is characterized by two distinct states, as modeled mathematically in Eq (3.1):

$$x_{t+1}^{ij} = \begin{cases} x_t^{ij} + n \times (1 + \sin(r)) \times x_t^{ij}, & p < r, \\ x_t^{ij} + n \times (2r - 1) \times x_t^{ij}, & else, \end{cases} \quad n = 0.05 \times e^{-2\times(\frac{t}{T})^2}, \tag{3.1}$$

where, x_t^{ij} and x_{t+1}^{ij} represent the position of the i-th black kite in the j-th dimensional space during the t-th and $t + 1$-th iterations, respectively; r is a random number uniformly distributed in the interval $[0, 1]$, and p is a constant; T denotes the maximum number of iterations, and t represents the current iteration.

3.1.2. Migration behavior

Inspired by bird migration behavior, the BKA incorporates a dynamic leader selection strategy. The mathematical model of migration behavior is presented in Eq (3.2):

$$x_{i+1}^{ij} = \begin{cases} x_t^{ij} + C(0, 1) \times (x_t^{ij} - L_t^j), & F_i < F_{ri}, \\ x_t^{ij} + C(0, 1) \times (L_t^j - m \times x_t^{ij}), & else, \end{cases} \quad m = 2 \times \sin(r + \pi/2), \tag{3.2}$$

where L_t^j denotes the position of the leader in the black-winged kite population in the j-th dimensional space during the t-th iteration; F_i represents the fitness value of the current individual in the t-th iteration, while F_{ri} indicates the fitness value of a randomly selected individual in the same iteration; $C(0, 1)$ is the standard Cauchy mutation operation [18], with its specific expression given by Eq (3.3) when the parameters are set as $\delta = 1$ and $\mu = 0$:

$$C(0, 1) = \frac{1}{\pi} \frac{1}{1 + x^2}, -\infty < x < \infty. \tag{3.3}$$

3.2. BKA improved by multiple strategies

Although the BKA enhances optimization capability and accuracy to some extent through dynamic leader selection and Cauchy mutation, deficiencies remain in balancing global exploration and local exploitation, often leading to entrapment in local optima. To address this, an IBKA is proposed, incorporating the following three enhancement strategies.

3.2.1. Combination of Sobol sequence with opposition-based learning

In swarm intelligence optimization algorithms, the quality of the initial population directly impacts search efficiency and optimization performance. To enhance the uniformity of the initial solution distribution within the solution space, an initial population with greater coverage should be generated [19]. The BKA employs a pseudo-random initialization strategy, which struggles to ensure uniform population distribution in the solution space, often resulting in searches being trapped in local regions. To address this, the Sobol sequence combined with a reverse learning strategy is introduced to generate the initial population.

The Sobol sequence, a low-discrepancy sequence, offers advantages such as uniform distribution and rapid convergence, effectively improving the initial population's distribution quality and the algorithm's global traversal capability [20]. The positions of the generated initial population are expressed as shown in Eq (3.4):

$$x_i = lb + R_n \times (ub - lb), \tag{3.4}$$

where lb is lower bound of the search interval, ub is upper bound of search interval, and R_n is a random number in the range [0,1] generated by Sobol sequence.

With a population size of 500 and a value range of $[0, 1]$, Figure 2 illustrates the distribution of initial populations generated by two strategies. The horizontal axis represents numerical values, while the vertical axis indicates the frequency of individuals within corresponding intervals. As depicted in Figure 2, the initial population generated using the Sobol sequence exhibits a more uniform distribution across the solution space compared to pseudo-random initialization.

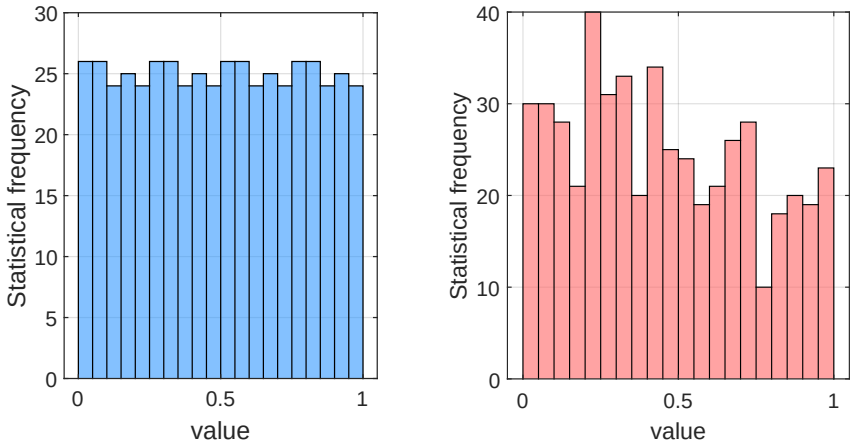

(a) Sobol distribution **(b)** Pseudo-random distribution

Figure 2. Initialization sequence distributions generated by different methods.

The initial population generated using the Sobol sequence demonstrates satisfactory distributional

uniformity; however, inadequate exploration of the solution space, particularly in reverse solution regions, may persist. To address this, an opposition-based learning (OBL) strategy [21] is integrated with the Sobol sequence to produce an initial population characterized by improved diversity and global representativeness.

The mathematical model for generating the reverse solution x_i' from an individual x_i is expressed as Eq (3.5):

$$x_i' = lb + ub - x_i. \tag{3.5}$$

In summary, the initial population is generated as follows: Initially, N candidate individuals are generated using the Sobol sequence to form population $S1$. Subsequently, a reverse population $S2$ is derived via the OBL strategy. Populations $S1$ and $S2$ are then combined into a single population S. Finally, the N individuals with the highest fitness values are selected to constitute the final initial population.

3.2.2. Adaptive spiral strategy

In the BKA, the position update associated with migration behavior constitutes the local search phase. To strengthen the algorithm's local exploitation capacity and enhance optimization precision, an adaptive spiral strategy [22, 23] is incorporated to refine the migration behavior.

The refined migration behavior is expressed in Eq (3.6) as follows:

$$\begin{gathered} x_{i+1}^{ij} = \begin{cases} x_t^{ij} + C(0,1) \times (x_t^{ij} - L_t^j), F_i < F_{ri}, \\ x_t^b + \overset{zl}{e} \times \cos(2\pi l) \times x_t^{ij}, else, \end{cases} \\ x_t^b = G \times e^{(\frac{x_t^{worse} - x_t^{ij}}{i^2})}, \\ z = e^{(h \cdot \cos(\pi(1 - \frac{t}{T})))}, \end{gathered} \tag{3.6}$$

where x_t^b represents the newly selected leader of current population; x_t^{worse} denotes the individual with the worst fitness value in current population; G is a random number following standard normal distribution; h is a constant and l is a random number within range [-1, 1].

3.2.3. Integration of the parrot optimizer

To improve the algorithm's adaptability and robustness in complex optimization environments, the foraging behavior strategy from the parrot algorithm [24] is incorporated. This strategy optimizes the search path, mitigating the risk of entrapment in local optima or prolonged exploration in inefficient regions, thus enhancing global exploration capacity and optimization efficiency.

The foraging behavior is expressed mathematically in Eq (3.7) as follows:

$$x_{i+1}^{ij} = (x_i^{ij} - L_t^j) \cdot Levy(dim) + c \cdot (1 - \frac{t}{T})^{\frac{2t}{T}} \cdot x_i^{mean}, \tag{3.7}$$

where x_i^{mean} denotes the average position of the current population of black-winged kites; $Levy(D)$ is *Levy* distribution, which models flight behavior of black-winged kites; and c is a random number uniformly distributed within [0, 1].

3.2.4. Flowchart of IBKA

The flowchart of IBKA is shown in Figure 3, and the process of the algorithm from initialization through iteration to the output of results is completely presented by it.

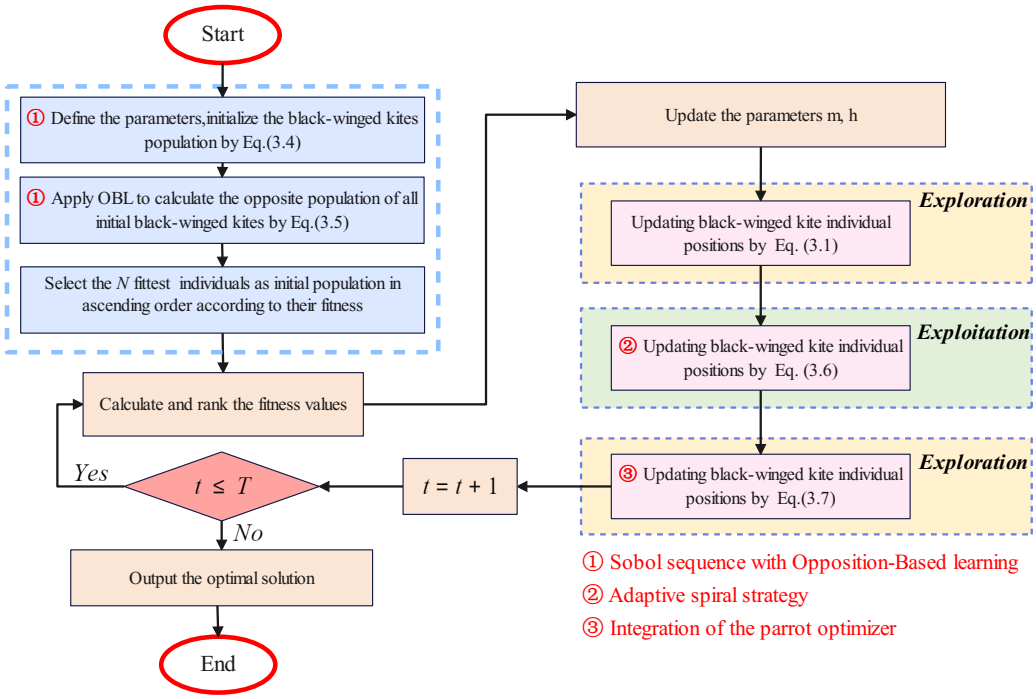

Figure 3. Flowchart of IBKA.

3.2.5. Time complexity analysis

The time complexity of an algorithm is a key indicator for assessing its efficiency [25]. This complexity is mainly influenced by three core processes: population initialization, fitness evaluation, and updates to the population's positions. For the original BKA, the time complexity is $O(N \times D \times T)$, where N corresponds to the number of individuals in the population, D represents the dimensionality of the optimization problem, and T denotes the maximum number of iterations. The time complexity of IBKA is analyzed as follows:

(1) The time complexity of initializing the black-winged kite population using the Sobol sequence is $O(N \times D)$. After incorporating this strategy, the overall time complexity of IBKA becomes $O(N \times D + N \times D \times T) = O(N \times D \times T)$, indicating no increase in time complexity. Additionally, the process of generating opposite solutions for the initial population produced by the Sobol sequence requires traversing the entire population, resulting in a time complexity of $O(N \times D + N \times D + N \times D \times T) = O(N \times D \times T)$.

(2) The adaptive spiral strategy is applied to migration behavior, replacing part of position update formula for migration. This modification suggests no additional increase in time complexity of IBKA.

(3) The foraging behavior of the parrot optimizer is integrated to introduce a global search strategy for the population. From the perspective of computational complexity, this strategy operates at the

population level and does not introduce additional computational loops or operations. Therefore, the total time complexity of IBKA remains $O(N \times D \times T)$.

In summary, the time complexity of IBKA can be expressed as $O(N \times D \times T)$, which is identical to that of the original BKA, indicating no increase in computational overhead.

3.3. Algorithm verification and analysis

3.3.1. Experimental design and parameter settings

For comparative experiments with the IBKA, ten algorithms are selected, encompassing the original BKA and a range of representative classical and contemporary optimization algorithms: parrot optimization (PO), dung beetle optimization (DBO) [26], osprey optimization algorithm (OOA) [27], arithmetic optimization algorithm (AOA) [28], aquila optimizer (AO) [29], sparrow search algorithm (SSA) [30], harris hawks optimization (HHO) [31], whale optimization algorithm (WOA) [22], and grey wolf optimizer (GWO) [32].

The performance of IBKA is evaluated against these ten algorithms on the IEEE CEC-2020 benchmark functions [33], with mean fitness value (Mean) and standard deviation (Std) as primary evaluation metrics. Optimal results are highlighted in bold to underscore IBKA's enhanced optimization capabilities. To ensure objectivity and statistical significance, Wilcoxon rank-sum tests and Friedman tests [34] are conducted. The Wilcoxon rank-sum test is performed at a significance level of $\alpha = 0.05$, based on computed p-values. In this framework, a "+" indicates that IBKA significantly outperforms the compared algorithm, "=" denotes no significant difference, and "–" signifies that the compared algorithm surpasses IBKA in performance.

To ensure the objectivity and fairness of the experiments, all tests were performed under consistent software and hardware environments. The experiments were conducted on a PC equipped with an Intel Core Ultra 5 125H processor operating at 2.50 GHz, 32 GB of RAM, and a 64-bit Windows 11 operating system, with MATLAB R2022a used for implementation. The parameters of the comparative algorithms were configured according to their respective original papers, and the specific parameter settings are provided in Table 1.

Table 1. Algorithm parameter settings.

Algorithm	Parameter settings
BKA	$P = 0.9$
PO	$\beta = 1.5$
DBO	$k = 0.1, b = 0.3, \alpha = -1$ or $\alpha = 1, s = 0.5$
OOA	$r_1 \in [0, 1]$
AOA	$\alpha = 5, MOP_{min} = 0.2, MOP_{max} = 1, \mu = 0.499$
AO	$\alpha = 0.1, \beta = 0.1, r_1 = 10$
SSA	$PD = 0.2, SD = 0.2, ST = 0.8$
HHO	$\beta = 1.5$
WOA	$b = 1, r_1, r_2 \in [0, 1]$
GWO	$a_{\max} = 2, a_{\min} = 0$
IBKA	$P = 0.9, h = 5, \beta = 1.5$

3.3.2. Results of experiment on IEEE CEC-2020

The IEEE CEC-2020 benchmark functions consists of 10 functions with varying dimensions and degrees of complexity. For all functions, the search space is $[-100, 100]$. The experimental setup included a population size of $N = 30$, a dimensionality of $D = 20$, and a total iteration limit of $T = 1000$. Each algorithm was ran independently 30 times to ensure reliability. The outcomes are summarized in Tables 2 and 3, and the corresponding average convergence trends are depicted in Figure 4.

Table 2. Results of CEC-2020 test functions.

Fun	Index	IBKA	BKA	PO	DBO	OOA	AOA	AO	SSA	HHO	WOA	GWO
F1	Mean	2.54E+05	5.14E+08	1.09E+08	9.12E+05	1.90E+10	1.67E+10	1.20E+07	**8.96E+03**	1.98E+06	2.80E+07	3.89E+08
	Std	1.74E+05	1.73E+09	1.97E+08	2.05E+06	5.59E+09	4.92E+09	8.16E+06	**7.20E+03**	5.89E+05	2.15E+07	4.37E+08
F2	Mean	2.32E+03	2.60E+03	2.90E+03	2.79E+03	3.78E+03	3.41E+03	2.46E+03	2.68E+03	2.44E+03	3.14E+03	**2.06E+03**
	Std	**2.84E+02**	4.35E+02	5.03E+02	3.43E+02	3.57E+02	3.75E+02	4.35E+02	3.84E+02	4.29E+02	4.93E+02	3.28E+02
F3	Mean	8.37E+02	8.44E+02	8.52E+02	7.91E+02	9.28E+02	9.09E+02	8.08E+02	9.07E+02	8.68E+02	8.82E+02	**7.58E+02**
	Std	2.55E+01	3.37E+01	2.71E+01	2.88E+01	3.64E+01	2.97E+01	**2.13E+01**	3.26E+01	3.07E+01	4.34E+01	2.29E+01
F4	Mean	**1.91E+03**	6.58E+03	1.92E+03	**1.91E+03**	3.26E+05	3.23E+05	1.92E+03	**1.91E+03**	1.92E+03	1.99E+03	**1.91E+03**
	Std	**2.61**	2.24E+04	2.08E+01	4.68	2.48E+05	1.93E+05	1.27E+01	3.56	3.82	1.06E+02	1.74E+01
F5	Mean	**6.28E+03**	2.22E+04	3.54E+05	3.33E+05	1.40E+07	2.22E+06	7.92E+05	1.13E+05	4.69E+05	3.46E+06	3.68E+05
	Std	**2.35E+03**	6.68E+04	3.27E+05	5.09E+05	2.80E+07	2.69E+06	7.42E+05	9.87E+04	3.25E+05	2.50E+06	3.76E+05
F6	Mean	**1.85E+03**	1.98E+03	2.05E+03	2.04E+03	2.37E+03	2.15E+03	1.97E+03	1.98E+03	2.04E+03	2.16E+03	1.88E+03
	Std	**8.52E+01**	2.13E+02	1.75E+02	2.37E+02	1.69E+02	1.97E+02	1.52E+02	1.75E+02	1.84E+02	2.16E+02	1.48E+02
F7	Mean	**6.37E+03**	9.68E+03	1.55E+05	1.05E+05	4.53E+06	1.88E+06	1.57E+05	6.52E+04	2.33E+05	5.05E+06	2.98E+05
	Std	**4.28E+03**	1.84E+04	1.13E+05	1.02E+05	3.28E+06	2.38E+06	1.31E+05	7.55E+04	1.99E+05	4.90E+06	4.85E+05
F8	Mean	2.31E+03	2.48E+03	2.32E+03	**2.30E+03**	4.43E+03	4.18E+03	2.31E+03	2.79E+03	2.38E+03	3.25E+03	2.58E+03
	Std	2.24	3.93E+02	5.44	4.71	6.97E+02	5.77E+02	**7.00E-01**	8.59E+02	3.58E+02	1.18E+03	6.75E+02
F9	Mean	2.91E+03	2.88E+03	2.87E+03	2.86E+03	3.58E+03	3.32E+03	2.86E+03	2.85E+03	2.93E+03	2.89E+03	**2.82E+03**
	Std	5.92E+01	8.26E+01	3.26E+01	4.50E+01	2.45E+02	2.10E+02	2.75E+01	7.85E+01	1.23E+02	7.45E+01	**1.66E+01**
F10	Mean	3.03E+03	3.16E+03	3.15E+03	3.07E+03	4.51E+03	4.31E+03	3.06E+03	**2.94E+03**	3.11E+03	3.18E+03	3.13E+03
	Std	8.27E+01	3.08E+02	6.71E+01	8.70E+01	3.39E+02	5.62E+02	8.48E+01	9.34E+01	6.43E+01	6.98E+01	**4.67E+01**
Friedman Rank		**2.5**	5.7	6.2	3.9	10.9	9.7	4.4	3.8	5.8	8.7	4.4
Final Rank		**1**	6	8	3	11	10	4	2	7	9	5

Table 3. Wilcoxon rank-sum test results for CEC-2020.

Fun	BKA	PO	DBO	OOA	AOA	AO	SSA	HHO	WOA	GWO
F1	4.06E-02	6.07E-11	2.61E-02	3.02E-11	3.02E-11	3.02E-11	3.02E-11	3.34E-11	3.02E-11	9.52E-04
F2	5.08E-03	8.88E-06	3.09E-06	3.02E-11	3.34E-11	3.71E-01	6.77E-05	4.38E-01	1.60E-07	6.91E-04
F3	4.83E-01	4.51E-02	2.78E-07	5.07E-10	1.86E-09	4.08E-05	5.00E-09	1.68E-04	1.75E-05	1.33E-10
F4	1.87E-07	1.60E-07	9.71E-01	3.02E-11	3.02E-11	3.16E-10	4.12E-01	5.00E-09	3.02E-11	1.41E-01
F5	6.10E-01	3.02E-11	2.19E-08	3.02E-11	3.02E-11	3.02E-11	7.77E-09	3.02E-11	3.02E-11	1.96E-10
F6	1.08E-02	9.53E-07	9.21E-05	3.34E-11	1.01E-08	5.26E-04	4.64E-03	2.60E-05	1.31E-08	5.79E-01
F7	9.35E-01	6.07E-11	1.61E-10	3.02E-11	3.02E-11	4.98E-11	2.39E-08	3.02E-11	3.02E-11	5.49E-11
F8	7.29E-03	1.20E-08	3.65E-08	3.02E-11	3.02E-11	2.49E-06	6.10E-03	3.16E-05	6.07E-11	2.32E-02
F9	9.05E-02	1.17E-02	1.77E-03	3.02E-11	4.98E-11	3.18E-04	7.20E-05	1.67E-01	4.73E-01	1.55E-09
F10	2.07E-02	9.76E-10	1.12E-01	3.02E-11	3.02E-11	3.87E-01	4.08E-05	2.60E-05	5.97E-09	1.31E-08
+/=/–	6/4/0	9/0/1	5/2/3	10/0/0	10/0/0	5/2/3	6/1/3	8/2/0	9/1/0	5/2/3

By analyzing the experimental results in Table 2, a comprehensive understanding of IBKA's performance on the test functions and its advantages or disadvantages compared to other algorithms can be obtained. On the unimodal function F1, IBKA shows significant improvement over BKA but performs slightly worse than SSA. For the multimodal function F2, IBKA ranks second only to GWO and significantly outperforms BKA. On F3, IBKA demonstrates performance comparable to BKA, exhibiting strong global search capabilities, though there is still room for improvement in escaping local optima. On the no-peak function F4, IBKA achieves optimal results alongside DBO, SSA, and GWO, showcasing excellent search stability and balance. For the hybrid functions F5-F7, IBKA achieves the best mean fitness values and the smallest standard deviations, highlighting its

significant advantages in complex multimodal problems. In the composite functions F8-F10, IBKA demonstrates overall superior performance. Although some results are slightly inferior to certain comparative algorithms, IBKA exhibits significant advantages in terms of overall fitness and mean performance metrics.

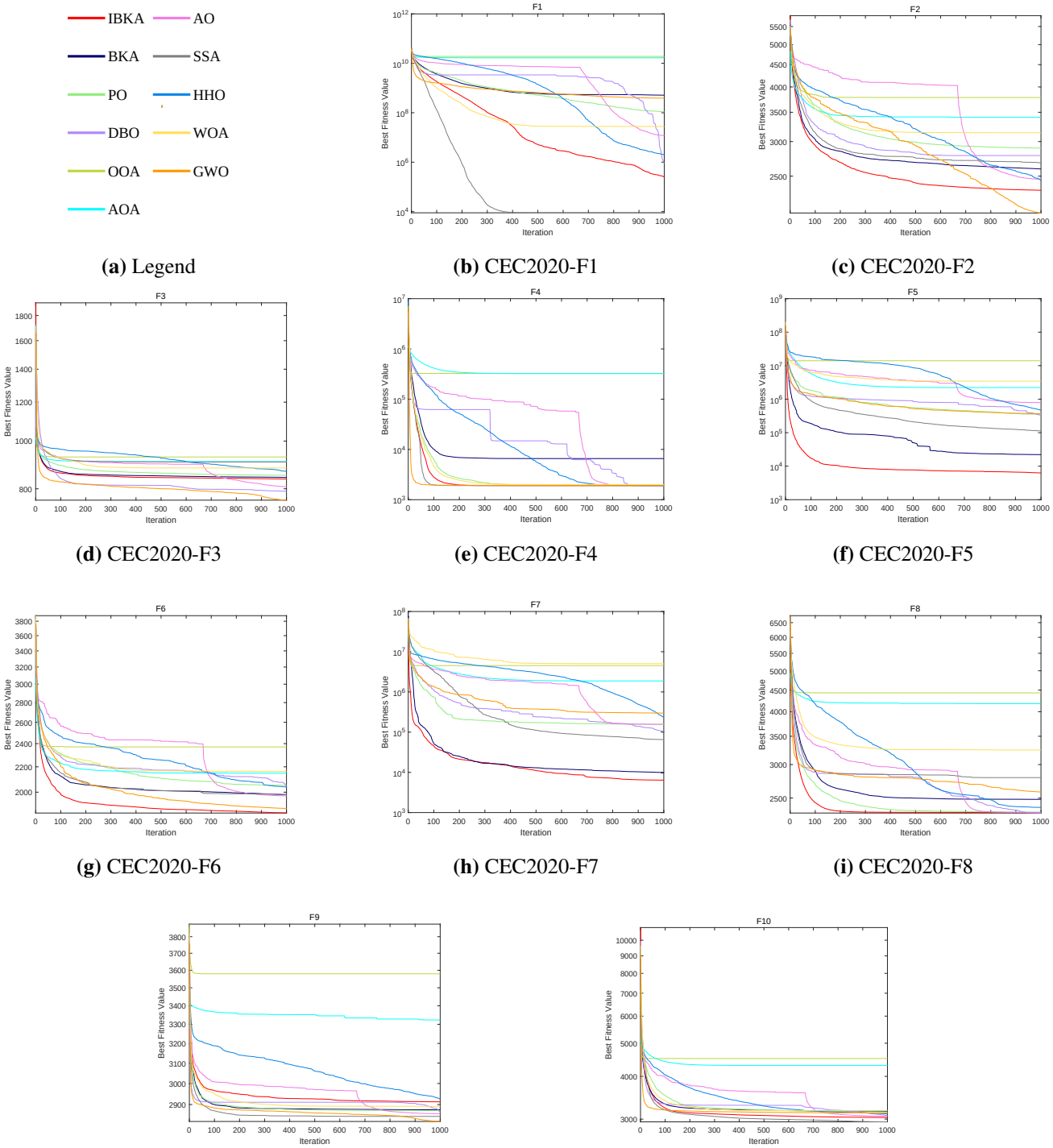

(a) Legend **(b)** CEC2020-F1 **(c)** CEC2020-F2

(d) CEC2020-F3 **(e)** CEC2020-F4 **(f)** CEC2020-F5

(g) CEC2020-F6 **(h)** CEC2020-F7 **(i)** CEC2020-F8

(j) CEC2020-F9 **(k)** CEC2020-F10

Figure 4. Comparison of convergence (IEEE CEC-2020).

Overall, IBKA demonstrates outstanding performance on most test functions, with particularly strong results observed in hybrid and composite functions. By comparing the average ranks and final ranks in Table 2, BKA ranks 6th, while IBKA achieves a significant improvement by ranking 1st overall. Although IBKA performs slightly worse than certain algorithms on certain multimodal and composite functions, it exhibits superior overall performance relative to BKA, reflecting its robustness and adaptability to various optimization problems.

To further compare the performance differences between IBKA and ten other algorithms on the IEEE CEC-2020 test suite, the Wilcoxon rank-sum test with a significance level of 0.05 was employed, with results presented in Table 3. The results indicate that IBKA performs exceptionally well on IEEE CEC-2020, particularly demonstrating significant advantages in complex and hybrid optimization problems (F6, F7, F8). IBKA significantly outperforms OOA and AOA across all test functions. Compared to DBO, AO, SSA, and GWO, IBKA exhibits superior performance on some functions but does not achieve comprehensive superiority, indicating room for optimization. In comparisons with PO, HHO, and WOA, IBKA demonstrates significant advantages in most test functions. Compared to BKA, IBKA shows significant improvements on six test functions, with comparable performance on the others. This suggests that IBKA achieves notable overall performance enhancements, though potential for improvement remains in certain optimization scenarios.

4. Degree reduction of DWBGB curves based on IBKA

In this section, the IBKA is utilized for degree reduction approximation of the DWBGB curve. The parameter settings are specified as follows: the coefficient τ is set to 0.8, λ is set to 230, the population size N is 30, and the maximum number of iterations T is 200.

4.1. Algorithm design

4.1.1. Initialize population

To address the degree reduction of the DWBGB curve, the IBKA is utilized to transform the n_1-th degree original curve $P(t)$ into an n_2-th degree reduced curve $Q(t)$. The optimization dimension for the center curve reduction is defined as $D = 2(n_2 + 1)$, while that for the radius function reduction is $D = n_2 + 1$. The parameters lb and ub represent the lower and upper bounds of the control disk for $P(t)$, respectively.

The initial population is generated using the Sobol sequence integrated with the opposition-based learning strategy, as outlined in Section 3.2.1. All experiments in this section are conducted with the endpoint preservation constraint, expressed as: $(Q_0) = (P_0), (Q_{n_2}) = (P_{n_1})$.

4.1.2. Fitness function

The control disks of the DWBGB curve are employed as the positional information for individuals. Throughout the algorithm's execution, individual positions are iteratively updated based on computed fitness values. Eqs (2.8) and (2.9) are utilized as the fitness functions for the IBKA in this study.

4.2. Algorithm steps

The implementation steps for addressing the DWBGB curve degree reduction approximation using the IBKA are outlined as follows:

Step 1. Relevant IBKA parameters, including population size N, dimension D, and maximum iteration count T, are initialized.

Step 2. The center curve $C_1(t)$ and radius function $R_1(t)$ of the n_1-th degree DWBGB curve $(P)(t)$ are computed using Eq (2.4).

Step 3. An initial population is generated based on Eqs (3.4) and (3.5) with individuals mapped to the control disks of $(Q)(t)$.

Step 4. Equation (2.8) is solved using IBKA to derive the center curve $C_2(t)$.

Step 5. The distance $dist(C_1(t), C_2(t))$ between curves $C_1(t)$ and $C_2(t)$ is calculated.

Step 6. Equation (2.9) is solved using IBKA to obtain the radius function $R_2(t)$.

Step 7. The degree reduction error between $(Q)(t)$ and $(P)(t)$ is computed using Eq (2.10).

Step 8. The above steps are executed independently 30 times, and the center coordinates and radius yielding the minimal degree reduction error are selected to derive the optimal n_2-th degree DWBGB curve $(Q)(t)$ using Eq (2.4).

4.3. Numerical examples

In this section, IBKA, BKA, GWO, HHO, and AO are evaluated through degree reduction approximation experiments on four numerical instances of the DWBGB curve. Each algorithm is independently executed 30 times, with metrics including mean error, standard deviation (Std) and minimum error computed. A comparative analysis is conducted, focusing on degree reduction error, convergence speed, and approximation accuracy. The optimal DWBGB curve derived from the 30 runs, along with its corresponding control disk center coordinates and radius, is reported.

4.3.1. Example 1

In this example, a 4th-degree DWBGB curve is specified, with its control disk center coordinates and radius defined by Eq (4.1), respectively. Five algorithms are utilized to perform a 1-degree reduction, resulting in a corresponding 3rd-degree DWBGB curve.

$$\begin{cases} p_0 = (0.4, 0.7), p_1 = (1.25, 2.6), p_2 = (2.6, 3.4), \\ p_3 = (3.95, 2.6), p_4 = (4.6, 0.7). \\ \{r_{1,i}\}_{i=0}^{4} = (0.04, 0.45, 0.5, 0.45, 0.04). \end{cases} \tag{4.1}$$

In Example 1, a 4th-degree DWBGB curve with location parameter $L = 2$, which corresponds to a Wang-Ball curve, is analyzed. The center coordinates and radius of the optimal 3rd-degree DWBGB curves derived by each algorithm are reported in Table 4, with degree reduction error results summarized in Table 5. Analysis reveals that the IBKA and GWO yield the lowest average errors, with standard deviations an order of magnitude smaller than those of other algorithms, indicating superior stability, with IBKA demonstrating the highest stability. Differences in minimum error among IBKA, BKA, GWO, and HHO are negligible, while AO exhibits slightly inferior performance. Overall, performance disparities in degree reduction approximation across the algorithms are minimal.

Table 4. Optimal center coordinates and radii of the control disks for Example 1.

Algorithm	Center coordinates	Radii
IBKA	$\{q_0 = (0.4, 0.7), q_1 = (1.3284, 2.9544), q_2 = (3.8737, 2.9353), q_3 = (4.6, 0.7)\}$	(0.0832,0.4976,0.4758,0.084)
BKA	$\{q_0 = (0.4, 0.7), q_1 = (1.3269, 2.9567), q_2 = (3.8751, 2.9356), q_3 = (4.6, 0.7)\}$	(0.087,0.4867,0.4817,0.0828)
GWO	$\{q_0 = (0.4, 0.7), q_1 = (1.3258, 2.9525), q_2 = (3.8753, 2.9407), q_3 = (4.6, 0.7)\}$	(0.0811,0.5066,0.4604,0.0894)
HHO	$\{q_0 = (0.4, 0.7), q_1 = (1.2587, 2.8883), q_2 = (3.9156, 3.0185), q_3 = (4.6, 0.7)\}$	(0.0998,0.3735,0.5979,0.0763)
AO	$\{q_0 = (0.4, 0.7), q_1 = (1.2927, 2.9705), q_2 = (3.8993, 2.8843), q_3 = (4.6, 0.7)\}$	(0.0672,0.6206,0.4188,0.0918)

Table 5. Degree reduction error results for Example 1.

Algorithm	Mean error	Std	Minimum error
IBKA	**5.99E-02**	**7.20E-04**	5.92E-02
BKA	6.04E-02	1.24E-03	5.91E-02
GWO	**5.99E-02**	7.79E-04	**5.90E-02**
HHO	8.18E-02	1.49E-02	6.04E-02
AO	8.33E-02	1.41E-02	6.68E-02

Figure 5 depicts the center curves and average convergence curves for the five algorithms. All algorithms produce center curves that closely approximate the original curve, with IBKA exhibiting notably faster convergence. Figure 6 illustrates the variation trends of $R_1(t) + dist(C_1(t), C_2(t))$ compared to $R_2(t)$ for each algorithm, while Figure 7 presents the optimal 3rd-degree DWBGB curves obtained.

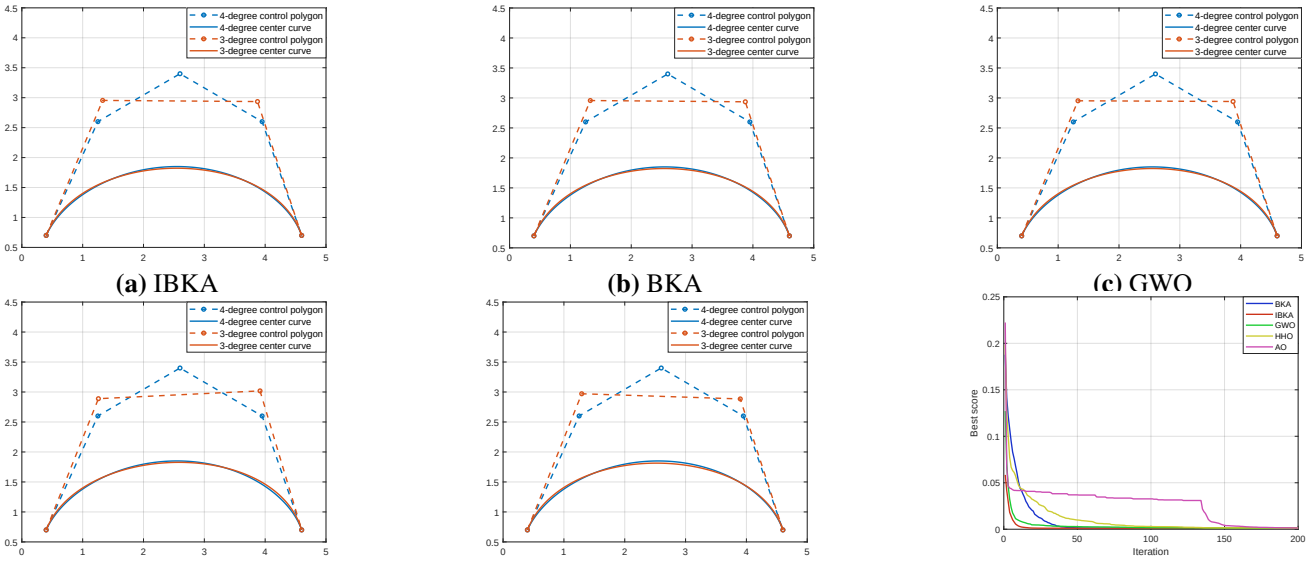

(a) IBKA **(b)** BKA **(c)** GWO **(d)** HHO **(e)** AO **(f)** Average convergence curves

Figure 5. Comparison of center curves and average convergence curves for Example 1.

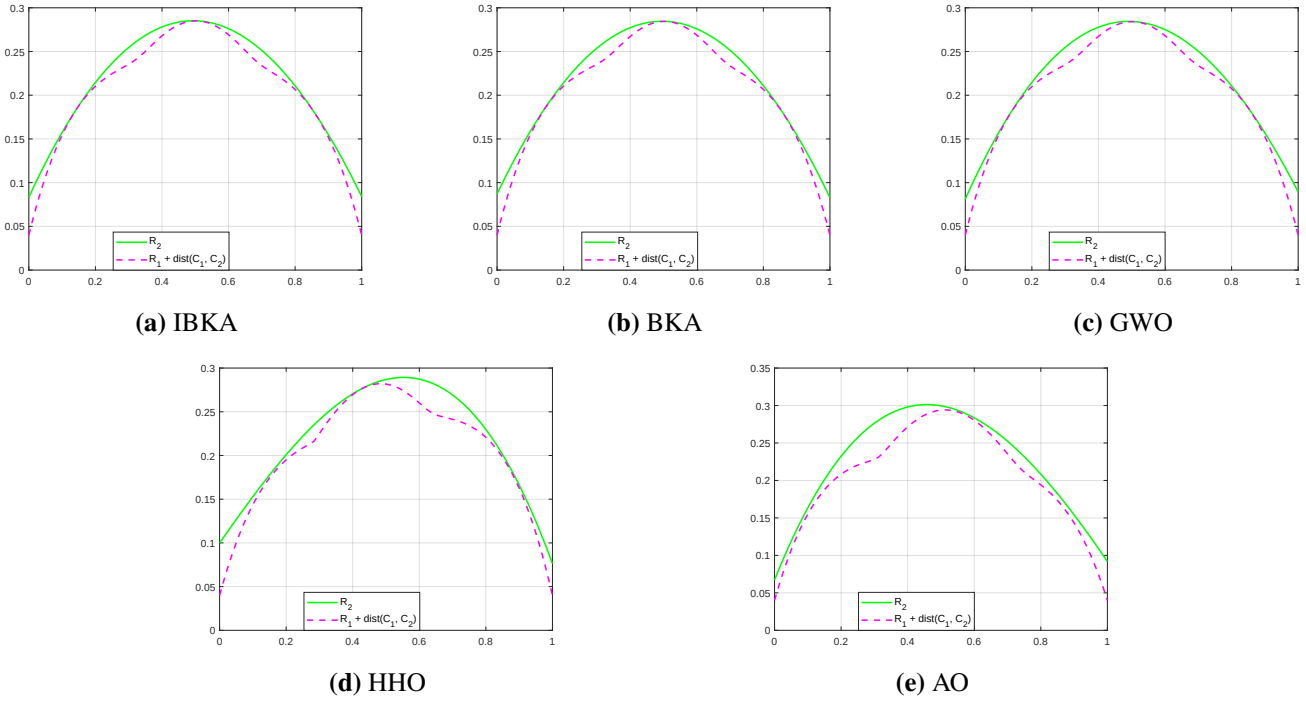

(a) IBKA **(b)** BKA **(c)** GWO

(d) HHO **(e)** AO

Figure 6. Comparison of $R_1(t) + dist(C_1(t), C_2(t))$ and $R_2(t)$ for Example 1.

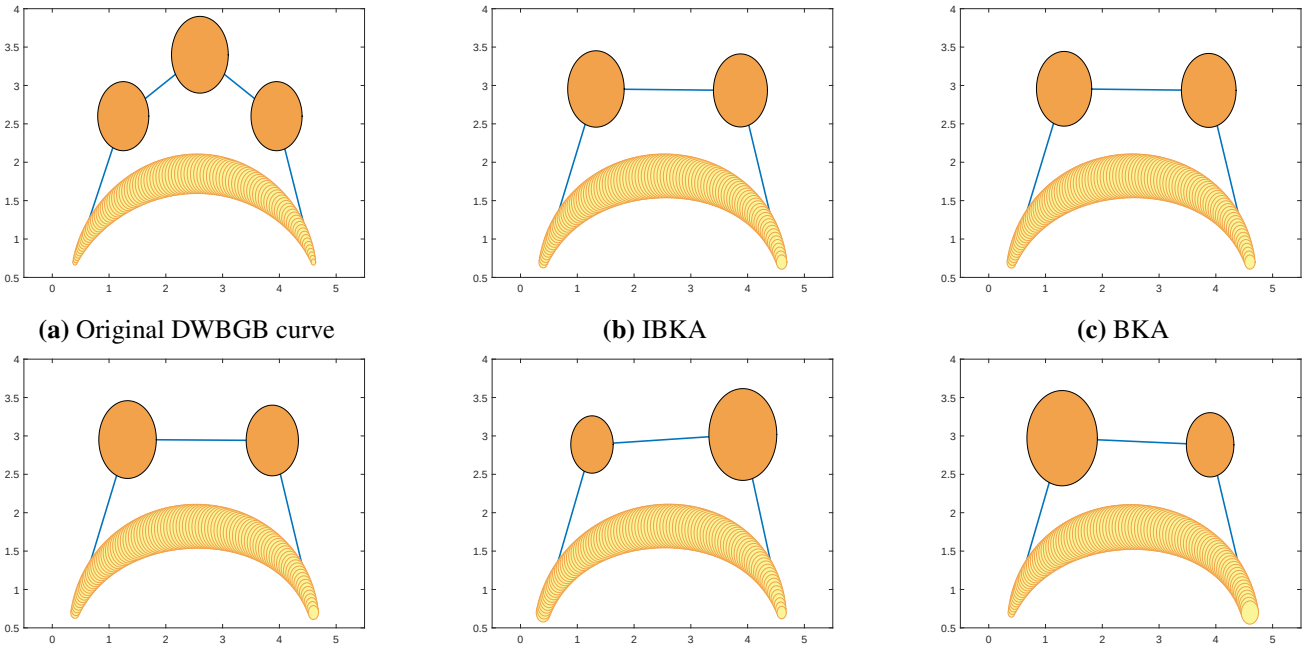

(a) Original DWBGB curve **(b)** IBKA **(c)** BKA

(d) GWO **(e)** HHO **(f)** AO

Figure 7. Comparison of the optimal DWBGB curves for Example 1.

In conclusion, the 1-degree reduction problem for this DWBGB curve exhibits low complexity, with

minor performance differences among algorithms. However, IBKA demonstrates a distinct advantage in stability.

4.3.2. Example 2

In this example, a 6th-degree DWBGB curve is given, with the center coordinates and radii of its control disks defined by Eq (4.2), respectively. After being solved using the degree reduction approximation algorithm, a 4th-degree DWBGB curve was employed to approximate the 6th-degree DWBGB curve.

$$\begin{cases} p_0 = (50, 110), p_1 = (80, 290), p_2 = (130, 300), p_3 = (190, 270), \\ p_4 = (240, 80), p_5 = (300, 110), p_6 = (330, 370). \end{cases} \tag{4.2}$$
$$\{r_{1,i}\}_{i=0}^{6} = (7, 5, 11, 14, 21, 7, 5).$$

In Example 2, a 6th-degree DWBGB curve with a location parameter $L = 2$, representing an intermediate form between a Bézier curve and a Wang-Ball curve, is analyzed. The center coordinates and radius of the optimal 4th-degree DWBGB curves derived by five algorithms are reported in Table 6, with corresponding degree-reduction error results summarized in Table 7. Analysis reveals that the GWO achieves the smallest minimum error, closely followed by the IBKA, with a marginal difference. For average error, IBKA outperforms the other four algorithms, exhibiting errors an order of magnitude lower than those of HHO and AO, indicating superior stability. The BKA demonstrates average error and standard deviation comparable to GWO, reflecting similar performance. In contrast, HHO and AO yield higher overall errors, indicating substantial potential for improvement in degree reduction approximation.

Table 6. Optimal center coordinates and radii of the control disks for Example 2.

Algorithm	Center coordinates	Radii
IBKA	$\{q_0 = (50, 110), q_1 = (60.9475, 316.8305), q_2 = (187.9745, 238.7919),$ $q_3 = (317.7251, 63.4743), q_4 = (330, 370)\}$	(9.5841,6.9178,12.2055 12.2055,14.2008,7.911)
BKA	$\{q_0 = (50, 110), q_1 = (57.3531, 308.4457), q_2 = (197.8819, 251.3074),$ $p_3 = (307.7093, 52.0561), p_4 = (330, 370)\}$	(8.6276,9.7441,13.1394, 7.8663,10.0581)
GWO	$\{q_0 = (50, 110), q_1 = (61.8005, 314.6084), q_2 = (187.3382, 242.3627),$ $q_3 = (318.0719, 59.855), q_4 = (330, 370)\}$	(9.3119,7.0223,12.3361, 12.4491,8.5743)
HHO	$\{q_0 = (50, 110), q_1 = (58.1208, 310.2553), q_2 = (201.5548, 253.8253),$ $q_3 = (301.1324, 47.1966), q_4 = (330, 370)\}$	(8.4792,12.0719,11.1067, 9.6921,10.6721)
AO	$\{q_0 = (50, 110), q_1 = (55.8869, 324.9537), q_2 = (184.4046, 213.5705),$ $q_3 = (326.8649, 94.3923), q_4 = (330, 370)\}$	(9.8128,11.1997,14.5498, 21.5913,7.4896)

Table 7. Degree reduction error results for Example 2.

Algorithm	Mean error	Std	Minimum error
IBKA	**3.88**	**6.01E-03**	3.87
BKA	8.62	3.75	4.29
GWO	7.34	3.79	**3.85**
HHO	2.25E+01	9.69	4.91
AO	1.40E+01	4.33	6.39

Figure 8 depicts the center curves and average convergence curves for the five algorithms. While approximation performance shows minimal variation among the algorithms, the IBKA demonstrates superior convergence speed and approximation accuracy. Figure 9 compares the alignment of $R_1(t) + dist(C_1(t), C_2(t))$ with the radius function $R_2(t)$ across the algorithms, while Figure 10 presents the optimal 4th-degree DWBGB curves derived by each algorithm. In the 2-degree reduction of the 6th-degree DWBGB curve, IBKA exhibits a distinct advantage, significantly surpassing other algorithms in both approximation accuracy and convergence speed.

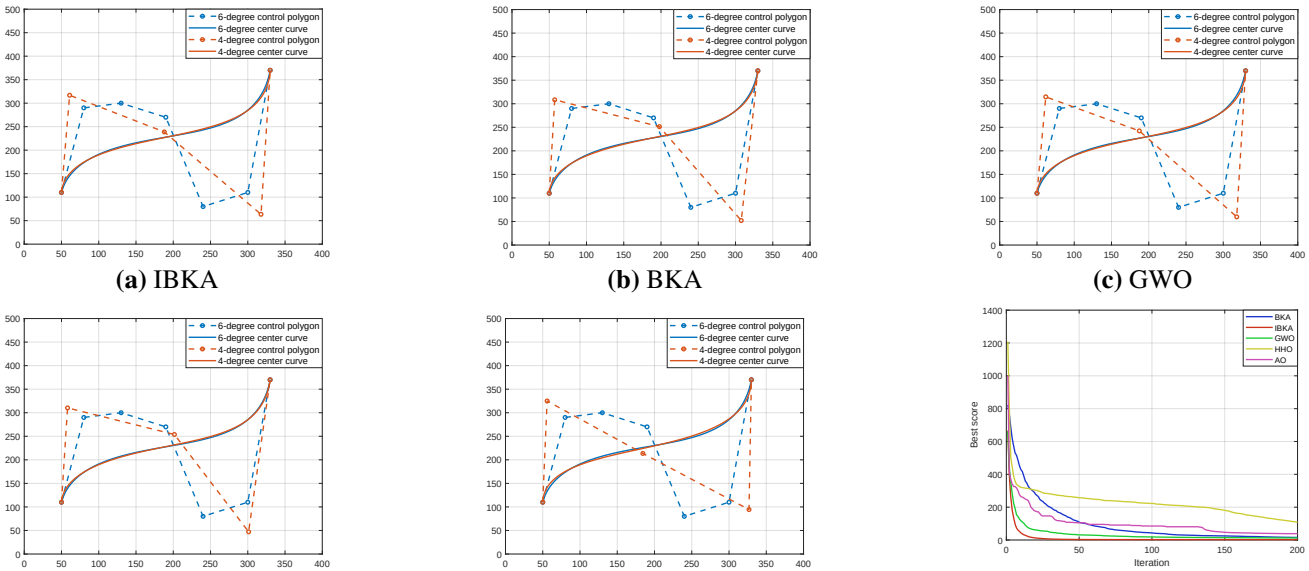

(a) IBKA **(b)** BKA **(c)** GWO **(d)** HHO **(e)** AO **(f)** Average convergence curves

Figure 8. Comparison of center curves and average convergence curves for Example 2.

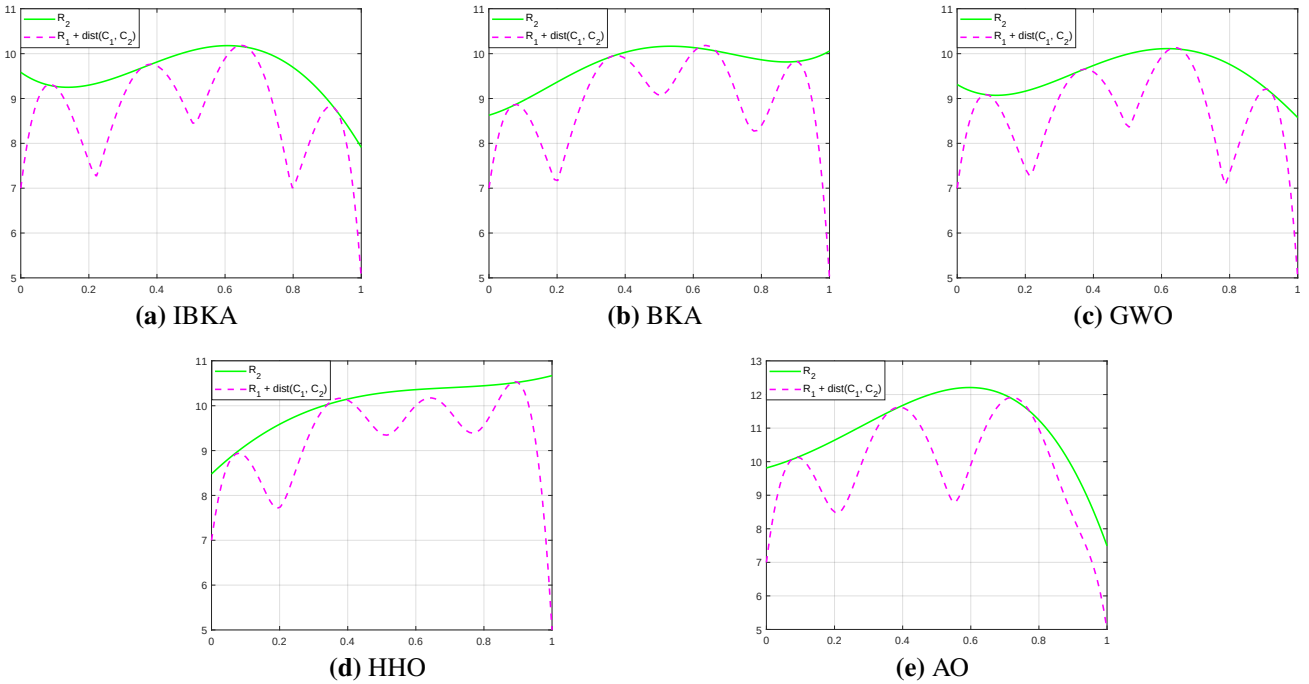

(a) IBKA **(b)** BKA **(c)** GWO **(d)** HHO **(e)** AO

Figure 9. Comparison of $R_1(t) + dist(C_1(t), C_2(t))$ and $R_2(t)$ for Example 2.

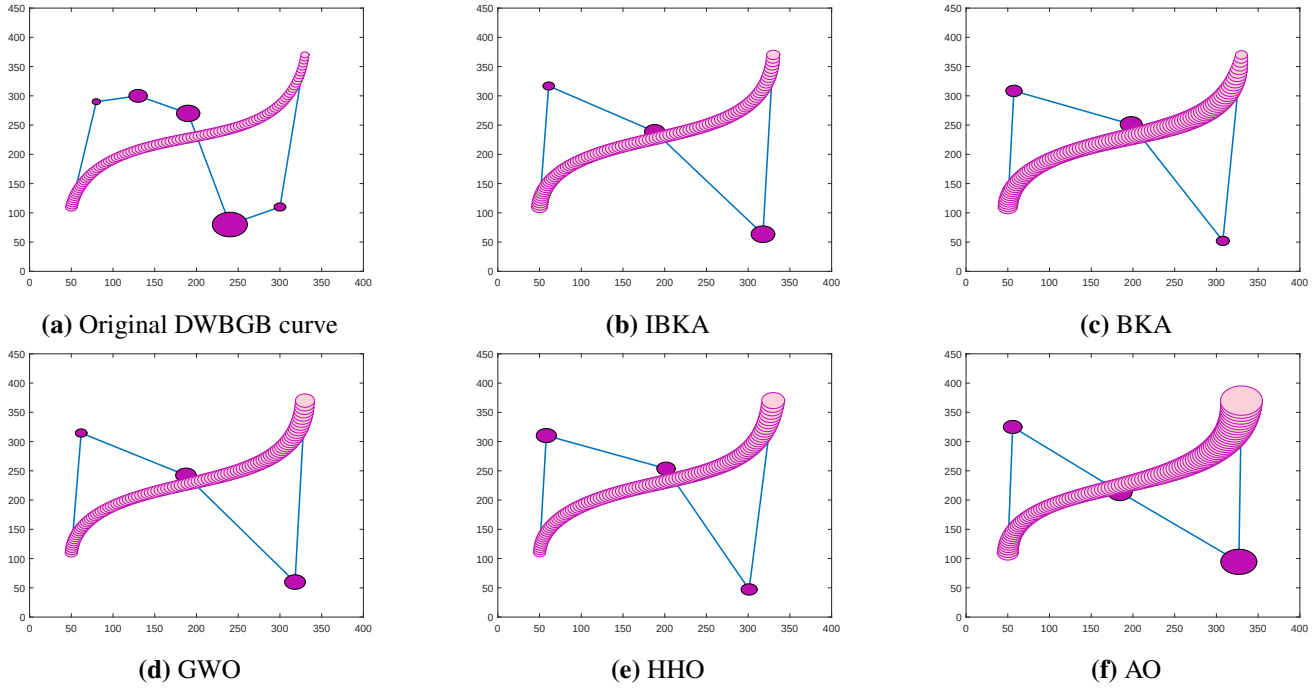

(a) Original DWBGB curve **(b)** IBKA **(c)** BKA

(d) GWO **(e)** HHO **(f)** AO

Figure 10. Comparison of the optimal DWBGB curves for Example 2.

4.3.3. Example 3

Given a 7th-degree DWBGB curve, center coordinates and radii of the control disks are provided in Eq (4.3), respectively. In this case, curve is reduced from 7th-degree to 4th-degree.

$$\begin{cases} p_0 = (1.6, 1.1), p_1 = (1.2, 2.2), p_2 = (1.7, 3.3), p_3 = (2.25, 3.9), \\ p_4 = (3.4, 4.1), p_5 = (4.5, 3.7), p_6 = (5.2, 2.4), p_7 = (4.8, 1.1). \\ \{r_{1,i}\}_{i=0}^{7} = (0.13, 0.17, 0.19, 0.15, 0.2, 0.3, 0.14, 0.13). \end{cases} \tag{4.3}$$

The location parameter of the 7th-degree DWBGB curve is set to $L = 0$, making the DWBGB curve a Bézier curve. Table 8 displays center coordinates and radii of the optimal 4th-degree DWBGB curves obtained by five algorithms, whereas Table 9 presents the corresponding degree reduction error results. IBKA demonstrates the best performance, achieving the smallest mean and minimum errors, as well as the highest stability. Although the minimum and mean errors of GWO are second only to IBKA, its standard deviation is the largest, suggesting the highest level of uncertainty in the algorithm. BKA and HHO exhibit similar performance, while AO shows the largest minimum and mean errors, demonstrating the poorest performance overall.

Figure 11 presents the center curves and average convergence curves obtained using the five algorithms. Compared to BKA, the best degree reduction effect for the center curve is achieved by IBKA, with faster convergence and a significant improvement in accuracy. Figure 12 compares $R_1(t) + dist(C_1(t), C_2(t))$ with the radius function $R_2(t)$, while Figure 13 illustrates the optimal 4th-degree DWBGB curves achieved after a 3-degree reduction. Therefore, IBKA demonstrates superior performance in the 3rd-degree approximation of the DWBGB curve, significantly improving both accuracy and convergence speed.

Table 8. Optimal center coordinates and radii of the control disks for Example 3.

Algorithm	Center coordinates	Radii
IBKA	$\{q_0 = (1.6, 1.1), q_1 = (1.1192, 2.9746), q_2 = (2.4397, 4.9449), q_3 = (5.4824, 3.5155), q_4 = (4.8, 1.1)\}$	(0.2128,0.1463,0.2107,0.2778,0.1304)
BKA	$\{q_0 = (1.6, 1.1), q_1 = (0.9109, 2.97), q_2 = (3.0296, 4.9949), q_3 = (5.1914, 3.3884), q_4 = (4.8, 1.1)\}$	(0.1667,0.1365,0.4732,0.2448,0.1912)
GWO	$\{q_0 = (1.6, 1.1), q_1 = (1.1038, 2.8699), q_2 = (2.4833, 5.1173), q_3 = (5.4707, 3.4135), q_4 = (4.8, 1.1)\}$	(0.1823,0.2395,0.1793,0.3006,0.1303)
HHO	$\{q_0 = (1.6, 1.1), q_1 = (0.9818, 3.0501), q_2 = (2.7487, 4.8106), q_3 = (5.4169, 3.741), q_4 = (4.8, 1.1)\}$	(0.1662,0.2141,0.2094,0.4753,0.1664)
AO	$\{q_0 = (1.6, 1.1), q_1 = (1.0834, 3.1463), q_2 = (2.5623, 4.4965), q_3 = (5.1996, 3.9684), q_4 = (4.8, 1.1)\}$	(0.221,0.13,0.2445,0.6073,0.1805)

Table 9. Degree reduction error results for Example 3.

Algorithm	Mean error	Std	Minimum error
IBKA	**4.96E-02**	**1.01E-02**	**3.17E-02**
BKA	2.09E-01	7.04E-02	1.18E-01
GWO	1.75E-01	1.21E-01	4.96E-02
HHO	2.43E-01	7.13E-02	1.19E-01
AO	2.65E-01	7.38E-02	1.60E-01

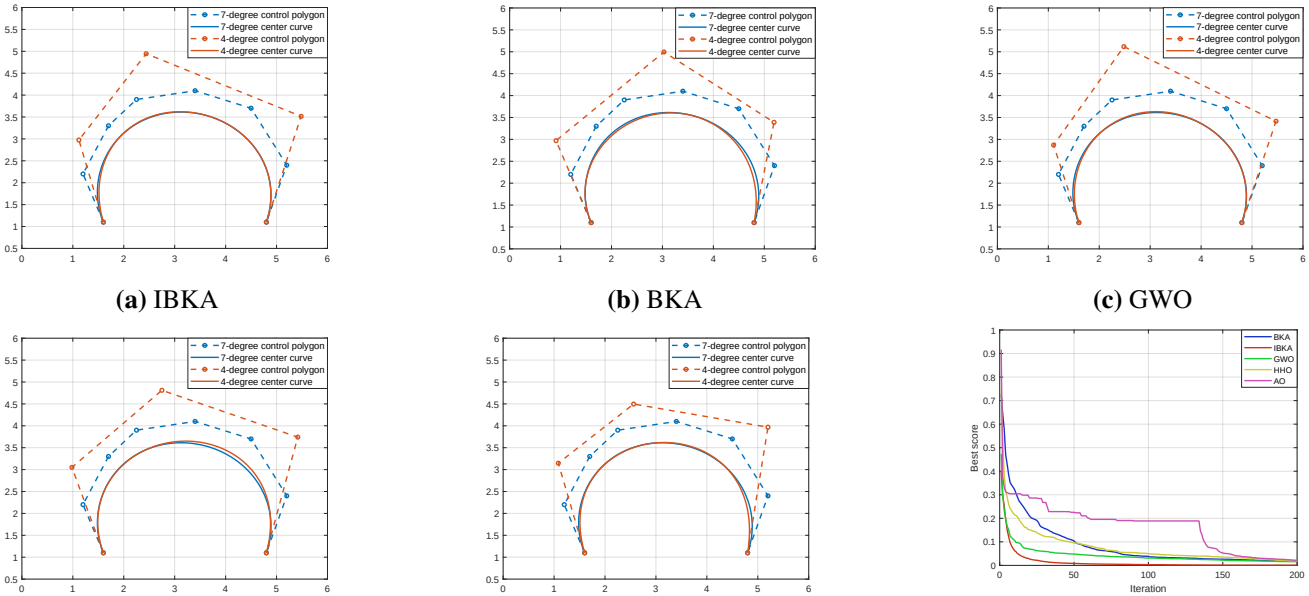

(a) IBKA **(b)** BKA **(c)** GWO

(d) HHO **(e)** AO **(f)** Average convergence curves

Figure 11. Comparison of center curves and average convergence curves for Example 3.

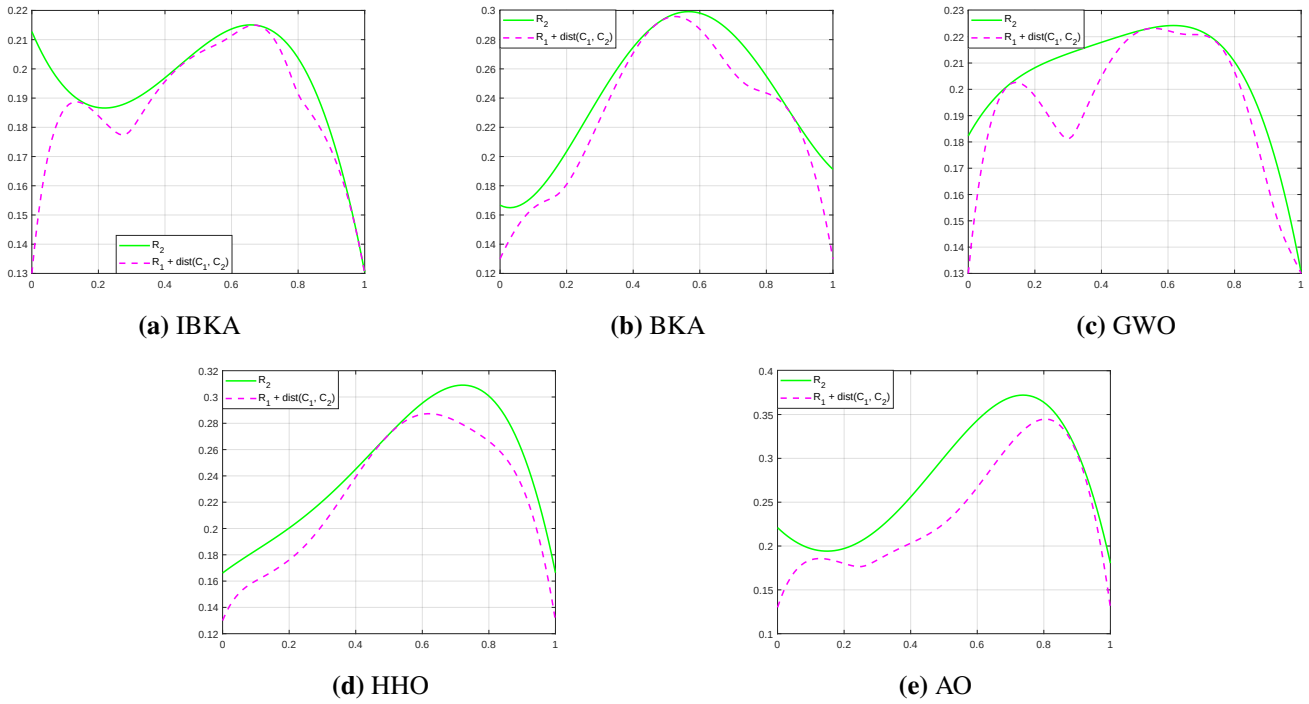

(a) IBKA **(b)** BKA **(c)** GWO

(d) HHO **(e)** AO

Figure 12. Comparison of $R_1(t) + dist(C_1(t), C_2(t))$ and $R_2(t)$ for Example 3.

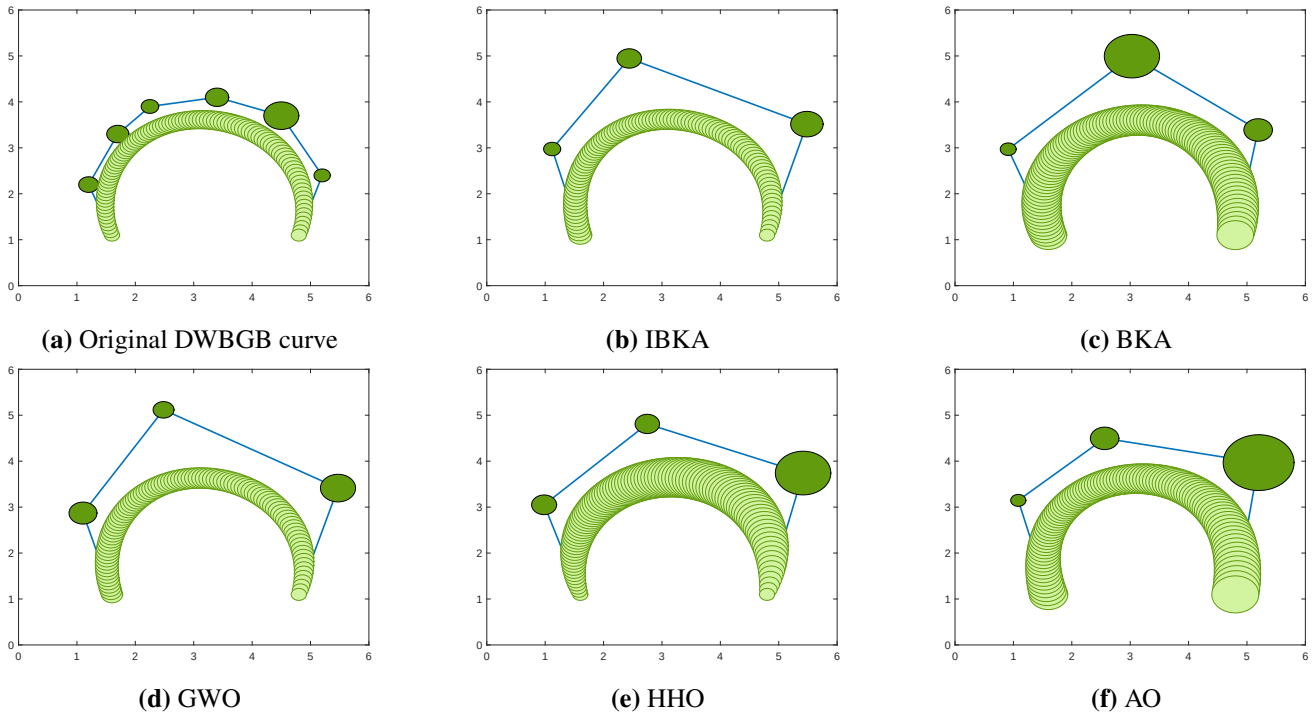

(a) Original DWBGB curve **(b)** IBKA **(c)** BKA

(d) GWO **(e)** HHO **(f)** AO

Figure 13. Comparison of the optimal DWBGB curves for Example 3.

4.3.4. Example 4

In this example, a 9th-degree DWBGB curve is given, with center coordinates and radii of its control disks defined by Eq (4.4), respectively. By solving the algorithm with the degree reduction algorithm, the 9th-degree DWBGB curve can be reduced to yield the 5th-degree DWBGB curve.

$$\begin{cases} p_0 = (0.4, 0.9), p_1 = (1.1, 6.7), p_2 = (2.5, 10), p_3 = (3.9, 6.9), p_4 = (4.3, 1.3), \\ p_5 = (5.5, 3.1), p_6 = (6.3, 6.7), p_7 = (7.7, 10), p_8 = (9.1, 6.9), p_9 = (9.8, 0.9). \\ \{r_{1,i}\}_{i=0}^{9} = (0.2, 0.7, 0.4, 0.19, 0.3, 0.3, 0.19, 0.4, 0.7, 0.2). \end{cases} \tag{4.4}$$

The location parameter of the 9th-degree DWBGB curve is set to $L = 4$, making the curve a Wang-Ball curve. Table 10 presents the center coordinates and radii of the five optimal 5th-degree DWBGB curves, while Table 11 lists the results of degree reduction errors. The error analysis demonstrates that IBKA attains the lowest values for mean error, standard deviation, and minimum error. Specifically, its mean error is an order of magnitude smaller than that of the other four algorithms, underscoring its enhanced stability. Although GWO exhibits slightly inferior performance compared to IBKA, its minimum error remains an order of magnitude lower than that of the remaining three algorithms.HHO outperforms BKA and AO overall, while BKA exhibits the largest error and the poorest degree reduction performance.

Table 10. Optimal center coordinates and radii of the control disks for Example 4.

Algorithm	Center coordinates	Radii
IBKA	$\{q_0 = (0.4, 0.9), p_1 = (1.2875, 7.6481), p_2 = (1.4383, 6.1111),$ $p_3 = (8.6583, 6.9836), q_4 = (8.9289, 7.6052), p_5 = (9.8, 0.9)\}$	(0.2605,0.6973,0.3284, 0.3364,0.7303,0.2404)
BKA	$\{q_0 = (0.4, 0.9), q_1 = (0.7316, 6.7946), q_2 = (3.3586, 9.4783),$ $q_3 = (7.2587, 2.5079), q_4 = (9.1849, 9.3227), q_5 = (9.8, 0.9)\}$	(0.2346,0.6368,0.794, 0.2846,0.6092,0.4117)
GWO	$\{q_0 = (0.4, 0.9), q_1 = (1.3248, 7.392), q_2 = (1.3698, 6.8519),$ $q_3 = (8.6676, 6.2757), q_4 = (8.9462, 7.8351), q_5 = (9.8, 0.9)\}$	(0.2611,0.5226,0.6539, 0.1928,0.755,0.2566)
HHO	$\{q_0 = (0.4, 0.9), q_1 = (1.0314, 7.8834), q_2 = (2.07, 6.3724),$ $q_3 = (8.1268, 5.336), q_4 = (9.0697, 8.4331), q_5 = (9.8, 0.9)\}$	(0.4404,0.1915,0.1914, 0.8353,0.2012,0.3979)
AO	$\{q_0 = (0.4, 0.9), q_1 = (1.6478, 7.7246), q_2 = (0.4927, 6.3474),$ $q_3 = (9.3008, 5.0828), q_4 = (8.9737, 8.8095), q_5 = (9.8, 0.9)\}$	(0.3213,0.5747,0.3253, 0.4159,0.3192,0.4693)

Table 11. Degree reduction error results for Example 4.

Algorithm	Mean Error	Std	Minimum Error
IBKA	**6.52E-02**	**5.45E-03**	**5.98E-02**
BKA	3.90E-01	1.39E-01	1.57E-01
GWO	1.97E-01	1.16E-01	6.32E-02
HHO	2.31E-01	6.61E-02	1.08E-01
AO	2.79E-01	9.76E-02	1.40E-01

Figure 14 compares central curves and average convergence curves for each algorithm. With respect to central curve reduction, the convergence speeds of IBKA and GWO are similar, but IBKA achieves

superior convergence accuracy. Figure 15 compares $R_1(t) + dist(C_1(t), C_2(t))$ and the radius functions $R_2(t)$ for each algorithm, and Figure 16 displays the optimal 5th-degree DWBGB curves. In conclusion, IBKA demonstrates the best degree reduction effect, yielding the closest DWBGB curve to the original one with the smallest error, further validating its advantages in terms of accuracy and stability.

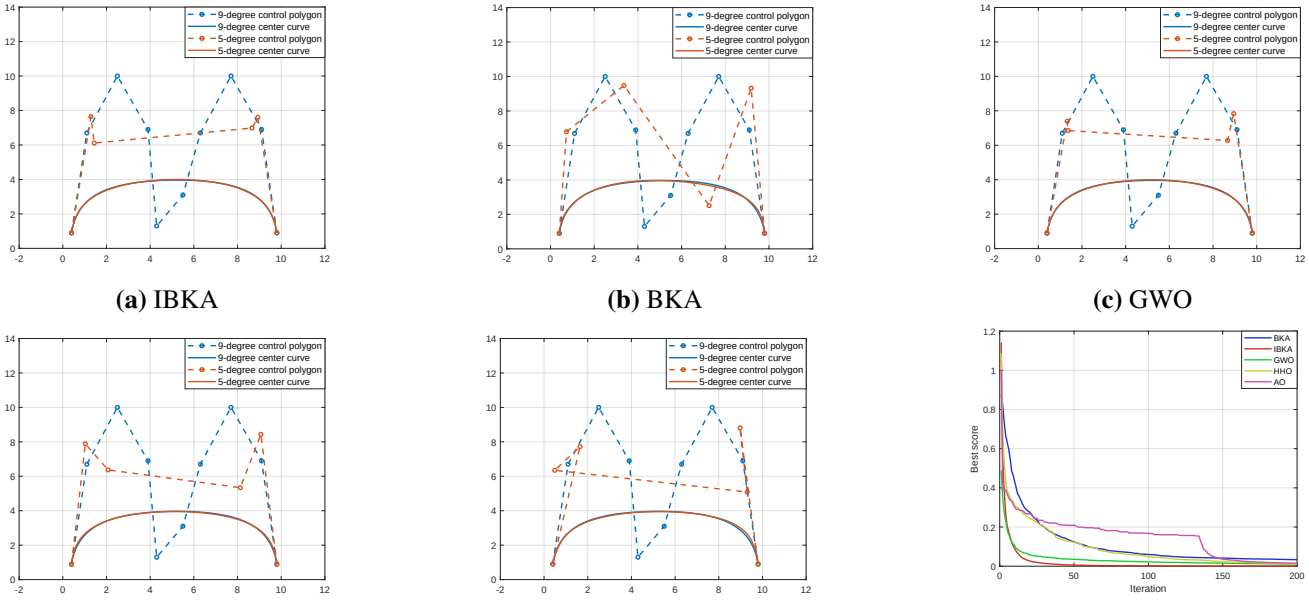

(a) IBKA **(b)** BKA **(c)** GWO

(d) HHO **(e)** AO **(f)** Average convergence curves

Figure 14. Comparison of center curves and average convergence curves for Example 4.

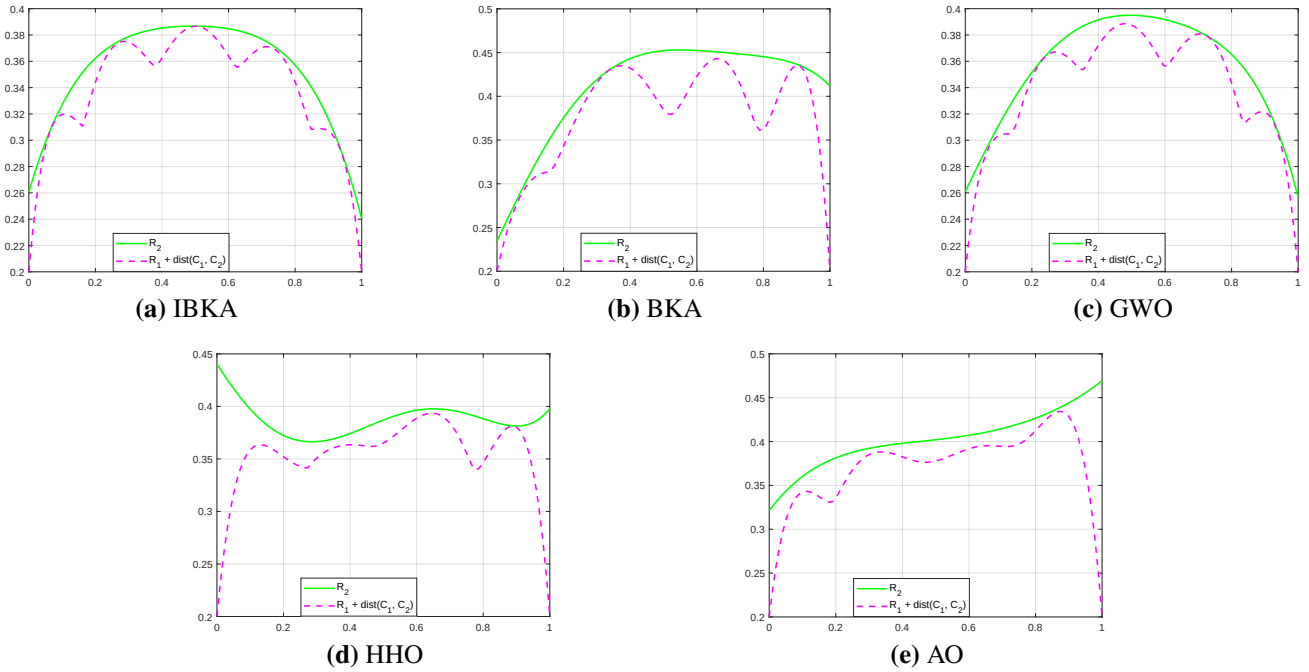

(a) IBKA **(b)** BKA **(c)** GWO

(d) HHO **(e)** AO

Figure 15. Comparison of $R_1(t) + dist(C_1(t), C_2(t))$ and $R_2(t)$ for Example 4.

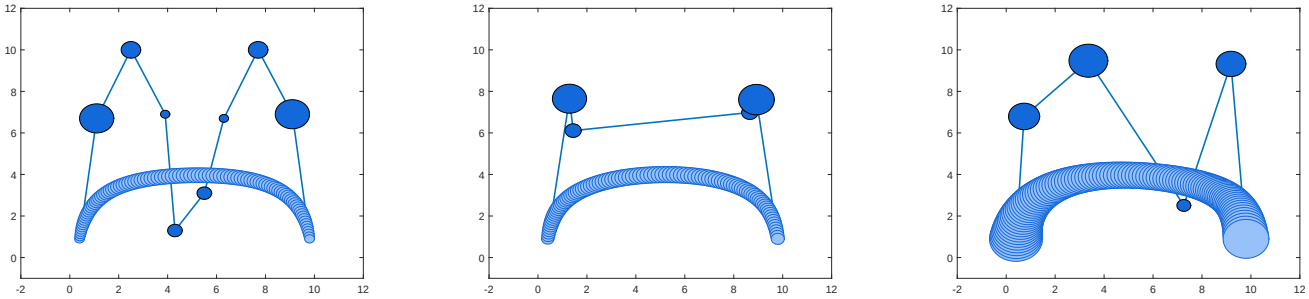

(a) Original DWBGB curve **(b)** IBKA **(c)** BKA

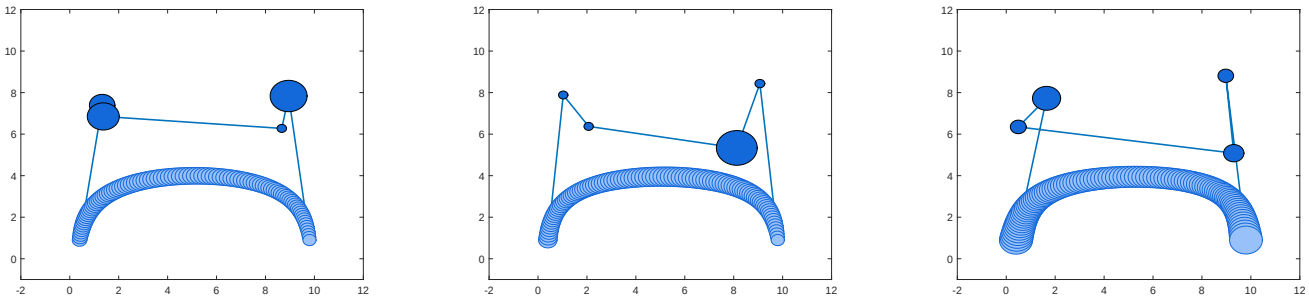

(d) GWO **(e)** HHO **(f)** AO

Figure 16. Comparison of the optimal DWBGB curves for Example 4.

5. Conclusions

This study addresses the degree-reduction approximation of DWBGB curves, integrating geometric properties such as Euclidean distance, curvature, and radius. Models for degree reduction approximation are developed, using control disk center coordinates and radius as decision variables, and a novel error metric for degree reduction is introduced. To optimize these models efficiently, an IBKA is proposed. Experiments on the IEEE CEC-2020 benchmark functions demonstrate that IBKA surpasses existing mainstream algorithms in computational efficiency, solution accuracy, and robustness, reflecting enhanced global optimization capabilities. Under endpoint preservation constraints, IBKA is evaluated against four other swarm intelligence algorithms across four DWBGB curve degree reduction instances. Results confirm IBKA's superior performance in both degree reduction accuracy and convergence stability.

The proposed approach not only effectively resolves the DWBGB curve degree reduction problem but also holds potential for application to broader geometric approximation domains, such as ball-based curves and surfaces, indicating significant practical utility.

Author contributions

Xia Wang: Methodology, Software, Writing-original draft; Feng Zou: Software, Formal analysis; Weilin Zhang: Data curation; Huogen Yang: Supervision, Conceptualization, Writing-review editing, Funding acquisition. Xia Wang and Feng Zou contributed equally to this work. All authors have read and approved the final version of the manuscript for publication.

Acknowledgments

This research is financially supported by the National Natural Science Foundation of China (12161043), Ganzhou City Guiding Science and Technology Plan Project (GZ2024ZSF874), Jiangxi Postgraduate Innovation Special Fund Project (YC2024-S528) and Postgraduate Innovation Special Fund Project of Jiangxi University of Science and Technology (XY2024-S051).

Conflict of interest

The authors declare that they have no conflicts of interest.

References

1. K. Kruppa, R. Kunkli, M. Hoffmann, A skinning technique for modeling artistic disk b-spline shapes, *Comput. Graph.*, **115** (2023), 96–106. https://doi.org/10.1016/j.cag.2023.06.030
2. S. Hu, G. Wang, T. Jin, Properties of two types of generalized ball curves, *Comput. Aided Design*, **28** (1996), 125–133. https://doi.org/10.1016/0010-4485(95)00047-X
3. W. Hongyi, Unifying representation of bézier curve and generalized ball curves, *Appl. Math. Chin. Univ.*, **15** (2000), 109–121. https://doi.org/10.1007/s11766-000-0016-5
4. J. Tan, Z. Fang, Degree reduction of interval generalized ball curves of Wang-Said type (Chinese), *Journal of Computer-Aided Design and Computer Graphics*, **20** (2008), 1483–1493.
5. G. Liu, G. Wang, Explicit multi-degree reduction of Said-Bézier generalized ball curves, *Journal of Software*, **21** (2010), 1473–1479. https://doi.org/10.3724/SP.J.1001.2010.00584
6. Y. Wang, Z. Li, Degree reduction of Wang-Bézier generalized ball curves (Chinese), *Journal of Graphics*, **37** (2016), 476–482. https://doi.org/10.11996/JG.j.2095-302X.2016040476
7. Q. Lin, J. Rokne, Disk Bézier curves, *Comput. Aided Design*, **15** (1998), 721–737. https://doi.org/10.1016/S0167-8396(98)00016-8
8. F. Chen, W. Yang, Degree reduction of disk Bézier curves, *Comput. Aided Design*, **21** (2004), 263–280. https://doi.org/10.1016/j.cagd.2003.10.004
9. Z. Liu, Y. Lyu, X. Liu, J. Xie, Degree reduction of disk q-Bézier curves (Chinese), *Journal of Computer-Aided Design and Computer Graphics*, **29** (2017), 860–867.
10. W. Wang, W. Tian, D. Xu, H. Zang, Arctic puffin optimization: a bio-inspired metaheuristic algorithm for solving engineering design optimization, *Adv. Eng. Softw.*, **195** (2024), 103694. https://doi.org/10.1016/j.advengsoft.2024.103694
11. F. Zou, X. Wang, W. Zhang, Q. Shi, H. Yang, Multi-degree reduction of Said-Ball curves and engineering design using multi-strategy enhanced Coati optimization algorithm, *Biomimetics*, **10** (2025), 416. https://doi.org/10.3390/biomimetics10070416
12. G. Hu, Y. Qiao, X. Qin, G. Wei, Approximate multi-degree reduction of SG-Bézier curves using the grey wolf optimizer algorithm, *Symmetry*, **11** (2019), 1242. https://doi.org/10.3390/sym11101242

13. H. Cao, H. Zheng, G. Hu, The optimal multi-degree reduction of ball Bézier curves using an improved squirrel search algorithm, *Eng. Comput.*, **39** (2023), 1143–1166. https://doi.org/10.1007/s00366-021-01499-0

14. G. Hu, R. Yang, G. Wei, Hybrid chameleon swarm algorithm with multi-strategy: a case study of degree reduction for disk Wang-Ball curves, *Math. Comput. Simulat.*, **206** (2023), 709–769. https://doi.org/10.1016/j.matcom.2022.12.001

15. L. Zhang, H. Wu, J. Tan, Dual bases for Wang-Bézier basis and their applications, *Appl. Math. Comput.*, **214** (2009), 218–227. https://doi.org/10.1016/j.amc.2009.03.079

16. Z. Fang, Degree reduction of interval and disk generalized ball curves of Wang-Said type, M. Sc Thesis, Hefei University of Technology, 2009.

17. J. Wang, W. Wang, X. Hu, L. Qiu, H. Zang, Black-winged kite algorithm: a nature-inspired meta-heuristic for solving benchmark functions and engineering problems, *Artif. Intell. Rev.*, **57** (2024), 98. https://doi.org/10.1007/s10462-024-10723-4

18. Y. Bao, C. Xing, J. Wang, X. Zhao, X. Zhang, Y. Zheng, Improved teaching-learning-based optimization algorithm with Cauchy mutation and chaotic operators, *Appl. Intell.*, **53** (2023), 21362–21389. https://doi.org/10.1007/s10489-023-04705-2

19. Y. Olmez, G. Koca, A. Sengur, U. Acharya, Chaotic opposition golden sine algorithm for global optimization problems, *Chaos Soliton. Fract.*, **183** (2024), 114869. https://doi.org/10.1016/j.chaos.2024.114869

20. A. Tharwat, W. Schenck, Population initialization techniques for evolutionary algorithms for single-objective constrained optimization problems: deterministic vs. stochastic techniques, *Swarm Evol. Comput.*, **67** (2021), 100952. https://doi.org/10.1016/j.swevo.2021.100952

21. P. Huang, Y. Zhou, W. Deng, H. Zhao, Q. Luo, Y. Wei, Orthogonal opposition-based learning honey badger algorithm with differential evolution for global optimization and engineering design problems, *Alex. Eng. J.*, **91** (2024), 348–367. https://doi.org/10.1016/j.aej.2024.02.024

22. S. Mirjalili, A. Lewis, The whale optimization algorithm, *Adv. Eng. Softw.*, **95** (2016), 51–67. https://doi.org/10.1016/j.advengsoft.2016.01.008

23. X. Tao, W. Guo, Q. Li, C. Ren, R. Liu, Multiple scale self-adaptive cooperation mutation strategy-based particle swarm optimization, *Appl. Soft Comput.*, **89** (2020), 106124. https://doi.org/10.1016/j.asoc.2020.106124

24. J. Lian, G. Hui, L. Ma, T. Zhu, X. Wu, A. Heidari, et al., Parrot optimizer: algorithm and applications to medical problems, *Comput. Biol. Med.*, **172** (2024), 108064. https://doi.org/10.1016/j.compbiomed.2024.108064

25. S. Liang, M. Yin, G. Sun, J. Li, H. Li, Q. Lang, An enhanced sparrow search swarm optimizer via multi-strategies for high-dimensional optimization problems, *Swarm Evol. Comput.*, **88** (2024), 101603. https://doi.org/10.1016/j.swevo.2024.101603

26. J. Xue, B. Shen, Dung beetle optimizer: a new meta-heuristic algorithm for global optimization, *J. Supercomput.*, **79** (2023), 7305–7336. https://doi.org/10.1007/s11227-022-04959-6

27. M. Dehghani, P. Trojovský, Osprey optimization algorithm: a new bio-inspired metaheuristic algorithm for solving engineering optimization problems, *Front. Mech. Eng.*, **8** (2023), 1126450. https://doi.org/10.3389/fmech.2022.1126450

28. L. Abualigah, A. Diabat, S. Mirjalili, M. Abd Elaziz, A. Gandomi, The arithmetic optimization algorithm, *Comput. Method. Appl. M.*, **376** (2021), 113609. https://doi.org/10.1016/j.cma.2021.113609

29. L. Abualigah, D. Yousri, M. Abd Elaziz, A. Ewees, M. Al-qaness, A. Gandomi, Aquila optimizer: a novel meta-heuristic optimization algorithm, *Comput. Ind. Eng.*, **157** (2021), 107250. https://doi.org/10.1016/j.cie.2021.107250

30. J. Xue, B. Shen, A novel swarm intelligence optimization approach: sparrow search algorithm, *Syst. Sci. Control Eng.*, **8** (2020), 22–34. https://doi.org/10.1080/21642583.2019.1708830

31. A. Heidari, S. Mirjalili, H. Faris, I. Aljarah, M. Mafarja, H. Chen, Harris hawks optimization: algorithm and applications, *Future Gener. Comp. Sy.*, **97** (2019), 849–872. https://doi.org/10.1016/j.future.2019.02.028

32. S. Mirjalili, S. M. Mirjalili, A. Lewis, Grey wolf optimizer, *Adv. Eng. Softw.*, **69** (2014), 46–61. https://doi.org/10.1016/j.advengsoft.2013.12.007

33. J. Liang, P. Suganthan, B. Qu, D. Gong, C. Yue, Problem definitions and evaluation criteria for the CEC 2020 special session on multimodal multiobjective optimization, Technical Report 201912. https://doi.org/10.13140/RG.2.2.31746.02247

34. M. Friedman, A comparison of alternative tests of significance for the problem of m rankings, *Ann. Math. Statist.*, **11** (1940), 86–92. https://doi.org/10.1214/aoms/1177731944

AIMS Press